HTSA-72-11

HS-801067

FEASIBILITY OF HIGH-RESOLUTION PULSE-ECHO TECHNIQUES FOR AUTOMOBILE TIRE INSPECTION

Robert P. Ryan

JUNE 1973

INTERIM REPORT

Prepared for
DEPARTMENT OF TRANSPORTATION
NATIONAL HIGHWAY TRAFFIC SAFETY ADMINISTRATION
Research Institute
Washington D C 20591

1. Report No. HS-801067	2. Government Accession No.	3. Recipient's Catalog No.
4. Title and Subtitle Feasibility of High-Resolution Pulse-Echo Techniques for Automobile Tire Inspection		5. Report Date June 1973 6. Performing Organization Code
7. Author(s) Robert P. Ryan		8. Performing Organization Report No. DOT-TSC-NHTSA-72-11.
9. Performing Organization Name and Address Department of Transportation Transportation Systems Center Kendall Square, Cambridge MA 02142		10. Work Unit No. R3402/HS303 11. Contract or Grant No.
12. Sponsoring Agency Name and Address Department of Transportation National Highway Traffic Safety Administration Research Institute Washington D C 20591		13. Type of Report and Period Covered Interim Report 14. Sponsoring Agency Code

15. Supplementary Notes

16. Abstract

This report presents ultrasonic A-scan reflection oscillograms and B-scan one-dimensional scanning displays for small sections of automobile tires, and for tire-like rubber and cord composite structures, using impulse excitation of 1-MHz and 5-MHz transducers. Adequate penetration and resolution are exhibited to permit depth characterization of structures and defects. Small reflections at bonding interfaces exhibit variations indicating a potential capability for detection of interface bonding anomalies in tires.

17. Key Words	18. Distribution Statement
Nondestructive Inspection Automobile Tires Ultrasonics	DOCUMENT IS AVAILABLE TO THE PUBLIC THROUGH THE NATIONAL TECHNICAL INFORMATION SERVICE, SPRINGFIELD, VIRGINIA 22151.

19. Security Classif. (of this report)	20. Security Classif. (of this page)	21. No. of Pages	22. Price
Unclassified	Unclassified	80	

PREFACE

The work described in this report was performed in the context of an overall program at the Transportation Systems Center. This program was designed to assess the utility of various nondestructive test techniques for evaluation of automobile tires and is sponsored by the Department of Transportation through the National Highway Traffic Safety Administration, Research Institute. The program supports government activities which promote traffic safety through improving reliability of the vehicle system.

Legal standards for tire safety have been established, based on performance tests of a destructive nature, and the NHTSA currently administers a program of testing for compliance with these safety standards. The primary objective of the program at TSC is to establish alternatives that are technically and economically preferable to the destructive test methods presently employed for such compliance testing.

CONTENTS

LIST OF ILLUSTRATIONS

LIST OF ILLUSTRATIONS (CONTINUED)

LIST OF TABLES

1. INTRODUCTION

This report presents the results of certain bench-top experiments designed to assess the potential of ultrasonic reflection (pulse-echo) techniques for nondestructive tire testing. The work has been performed as part of an overall investigation of nondestructive testing techniques for automobile tires being conducted at the Transportation Systems Center of the Department of Transportation under sponsorship of the National Highway Safety Administration.[1]

Reflection signal oscillograms (A-scans) and small-scale one-dimensional scanning displays (B-scans) are presented for small sections cut from actual tires, and for rubber-cord composite specimens made in our laboratory from actual tire component materials. These data provide a basis for estimating the capabilities of tire inspection systems utilizing reflection techniques. A separate report[2] will discuss design considerations for practical inspection systems, ranging from a developmental system expected to have a capacity of several tires per hour, to automated multi-channel systems which could process several hundred tires per hour.

While reflection techniques have been previously advocated for tire testing[3], much of the recent prior work has been limited to through-transmission techniques.[4,5] This situation is surprising, since reflection techniques are generally preferred in ultrasonic testing.

A reflection measurement provides a great deal more useful information than a through-transmission measurement. Since the time axis measures the round-trip travel time of the acoustic signal, i.e., the depth from which the echo has been returned, the reflection signal yields information characterizing the structure and condition of the object throughout its volume. In contrast, a transmission measurement gives only the total

loss in propagation over some specified path through the object. No information is available as to where the loss may have occurred and it is even possible that variations in the efficiency of coupling of the sound into the tested object will be mistaken for internal defects.

Reflection techniques offer certain inherent practical advantages, since access to only one surface is required. Since this surface can be the outside surface, measurements can be conveniently made on mounted and inflated tires, thereby providing possibilities for tire inspection on vehicles. Furthermore, the use of a liquid for acoustic coupling (by far the most convenient approach) requires only that the tire be wet on the outside, a normal condition in service.

However, a much more important consideration is that reflection techniques offer a fundamental capability for detecting relatively minor variations in interface conditions which are likely to be associated with weak bonding. This capability is essentially nil with a through-transmission technique, simply because the percentage of energy reflected at well-bonded interfaces is normally small. A small change in conditions at the interface will be readily observable if the resulting change in the small reflected signal is measured directly, whereas the percentage change in the transmitted signal will be orders of magnitude smaller. For example, if 1% of the incident energy is being reflected at an interface, a change in the reflected energy by one part in ten will be accompanied by a change in transmitted energy of only one part in a thousand.

The fact that earlier workers have tended to favor through-transmission methods in spite of the greater power of reflection techniques can probably be attributed in part to difficulties in achieving the required thickness resolution at the modestly low ultrasonic frequencies which must be used. However, rather considerable advances in transducer design have been made since about 1969.[6] Using modern techniques, adequate resolution at frequencies providing adequate penetration is not a serious problem.

A continuing legitimate reason for disfavor is that reflection techniques are inherently more complex. The additional complexity arises principally in two areas. First, for optimum results, the transducer must be aligned perpendicular to the laminar interfaces of interest. Secondly, the richer information content of the reflection signals increases the complexity of data interpretation. In production applications of ultrasonic testing, the data interpretation problem is routinely solved by use of various kinds of electronic signal processing and the production of graphic displays synchronized to mechanical scanning of the object tested. The separate report on design of tire inspection systems[2] will discuss means of implementing appropriate scanning and display techniques while simultaneously dealing with the transducer alignment problem. It is concluded that the inherent complexities of reflection techniques can be dealt with through straightforward established engineering approaches.

Nevertheless, the costs of complexity are real enough, and if it can be assumed that one need only detect rather gross structural defects, the simpler transmission measurement will suffice. For example, outright separations are essentially opaque even to quite low-frequency ultrasound, and are readily detected with a simple air-coupled through-transmission system operating at 25 kHz.[1] However, if it is desired to search for other less obvious (but perhaps more important!) causes of tire failure, use of reflection techniques is essential to utilize the full capabilities of ultrasound for measuring variations in component thicknesses, revealing changes in materials properties, and detecting evidence of weaknesses in interface bonding.

The data presented in this report are chosen to illustrate the capabilities of high-resolution pulse echo methods both for detection of gross structural anomalies (such as outright separations, dimensional irregularities, misplacement of reinforcing materials, etc.) and for detection of subtle anomalies of interface bonding. For the reader already generally familiar with ultrasonic testing techniques, advance reference to Figure 13 will confirm immediately that resolution and penetration can be

simultaneously adequate. Similarly, Figures 18, 20, 25, and 27 will show that certain scanning-display techniques are available which will clearly reveal small subsurface irregularities even in the presence of the complex background of internal structure and external relief present in tires. For the reader with less prior familiarity, or with more immediate motivation or interest, the material to follow taken in the order presented will provide a somewhat tutorial explanation of the techniques employed, illustrated first by reflection signals obtained in simple cases involving plane interfaces, followed by discussion of the results obtained on a variety of slab specimens and samples cut from tires.

2. HIGH-RESOLUTION REFLECTION TECHNIQUES

2.1 FUNDAMENTALS

The essential elements of a pulse-echo ultrasonic system are indicated in Figure 1. A pulse generator excites a piezoelectric element in the transducer, causing it to generate an acoustic pulse, which is radiated into the acoustic buffer or coupling medium, and thence into the object to be tested. Waves reflected from interfaces or inhomogeneities return to the same transducer, which now acts as a receiver, permitting the reflection signal to be displayed on the oscilloscope. The clipping circuit minimizes overload of the oscilloscope amplifiers by the drive pulse applied to excite the transducer, which typically will be several hundred volts. The returning echo signals of interest are typically only a few millivolts in amplitude, and are not appreciably attenuated by the clipping circuit, as they remain below the threshold voltage of the diodes.

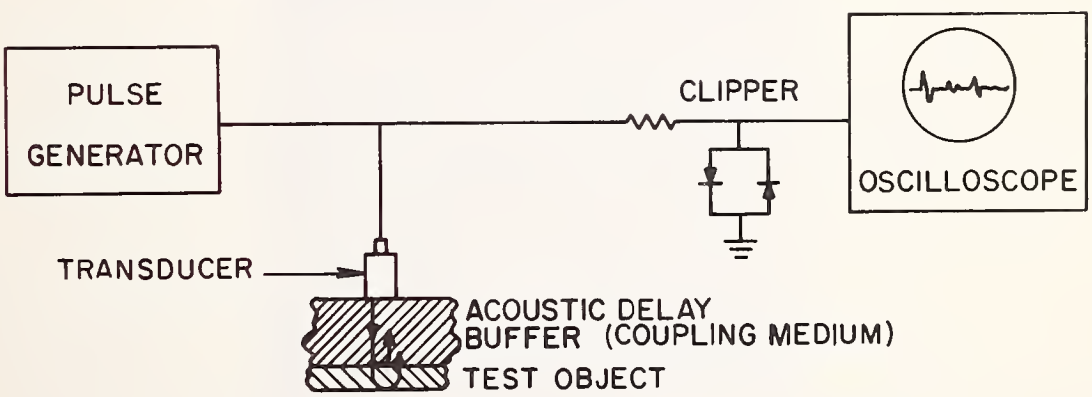

Figure 1. Basic Pulse-Echo Reflection System

In the usual applications where high sensitivity is commonly required for detection of small flaws, an RF pulse generator is frequently employed to excite the transducer at its resonant frequency, and a tuned receiver is used for optimum reception of the

resulting narrow-band pulse. Such pulses, however, are entirely too long to be of much use in tire testing. For example, the wavelength of 1-MHz ultrasound in tire rubber is about 1.6 mm, and therefore a pulse, consisting of say ten cycles, would be ten wavelengths, or 1.6 cm long. In typical tire structures, reflections from the front face and back face would overlap and hopelessly obscure any returns from interfaces in between, whether normal or abnormal.

For high-resolution in the thickness dimension, an unrectified broad-band receiving system is preferred, and the transducer is impulse-excited by a dc pulse, so that the outgoing acoustic pulse is limited in bandwidth only by the resonance properties of the transducer itself. In order that this resonance be as broad as possible, the piezoelectric element is bonded to a backing material. This material is ordinarily made highly absorptive to minimize interference from subsequent reflections from within the backing.[6]

Figure 2 illustrates the reflection signal seen on the oscilloscope when the transducer is in contact with a homogeneous material, in this case a 2"-thick flat plate of Plexiglas plastic. (As will be discussed later, "contact" is augmented by a thin film of some liquid (here propylene glycol) which wets both surfaces and excludes air.) At the beginning of the trace, the oscilloscope is overloaded by the so-called "main-bang" or drive pulse applied to excite the transducer, since this pulse is not completely isolated from the receiving circuitry. As the amplifiers recover and the oscilloscope trace returns to the base line, a number of small oscillations are seen caused by reflections of the inward-radiated pulse from within the transducer backing. At B (36 microseconds) we see the first round-trip reflection from the back face of the Plexiglas, and at C (72 microseconds) we see a pulse which has made a second round trip through the Plexiglas plate, after having been partially reflected when it first returned to the transducer/Plexiglas interface.

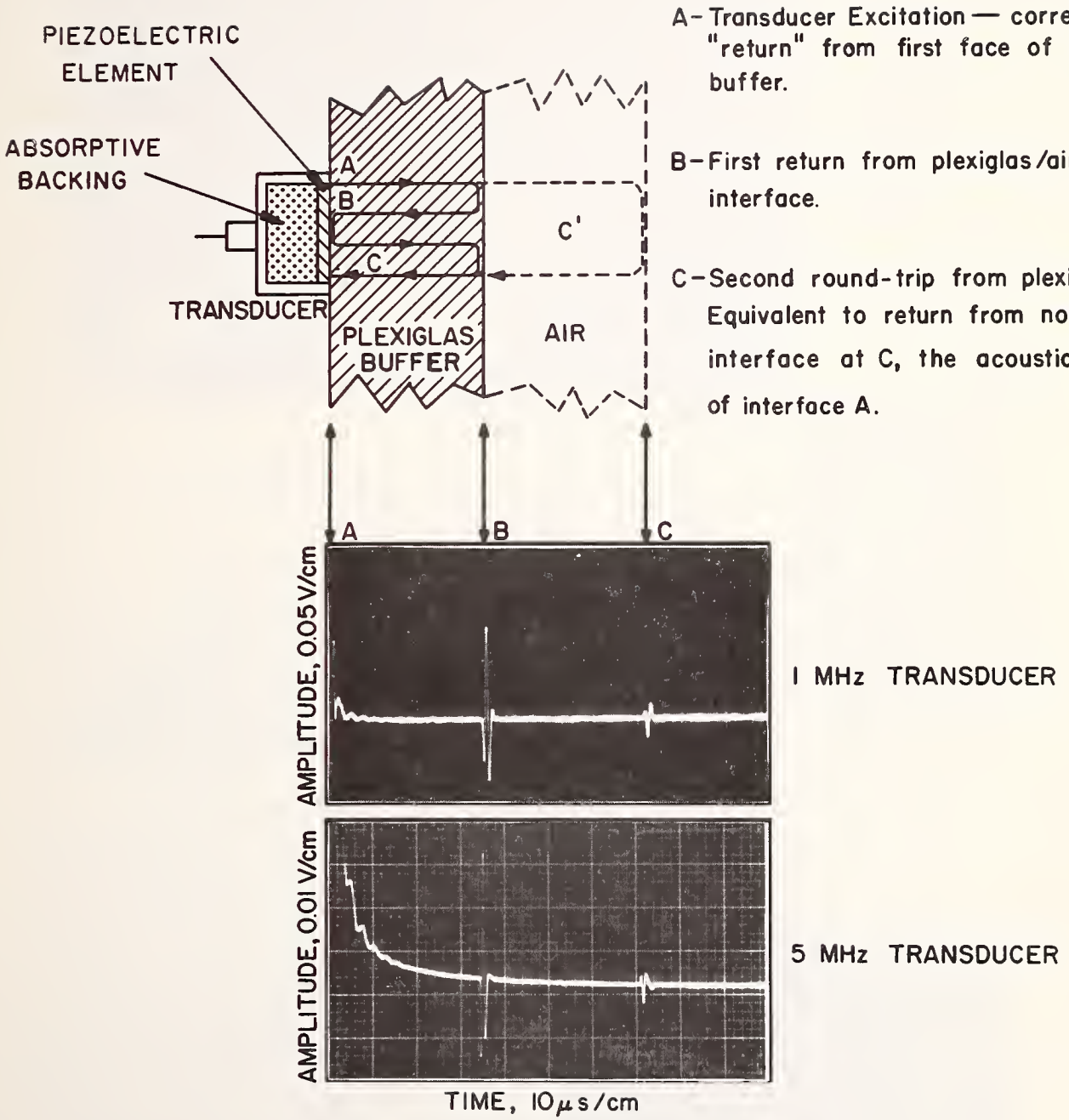

Figure 2. Reflections from 2-inch Plexiglas Acoustic Delay Buffer

Figures 3 and 4 illustrate the use of the buffered contact technique to examine a thin sample. A thin sheet of carcass type rubber 0.083" thick has been placed in wetted contact with the Plexiglas buffer, as shown in figure 4. In figure 3, the lower trace is the same as the previous 1-MHz trace shown in figure 2, except that the time scale has been expanded by a factor of two. In place of the simple one-and-one-half cycle pulse previously seen at B, reflected from the simple, plain Plexiglas/air boundary, we now see the first of a group of pulses (B, C, D,...) corresponding to multiple reflections from the sample. The acoustic delay provided by the round trip travel time in the buffer permits these

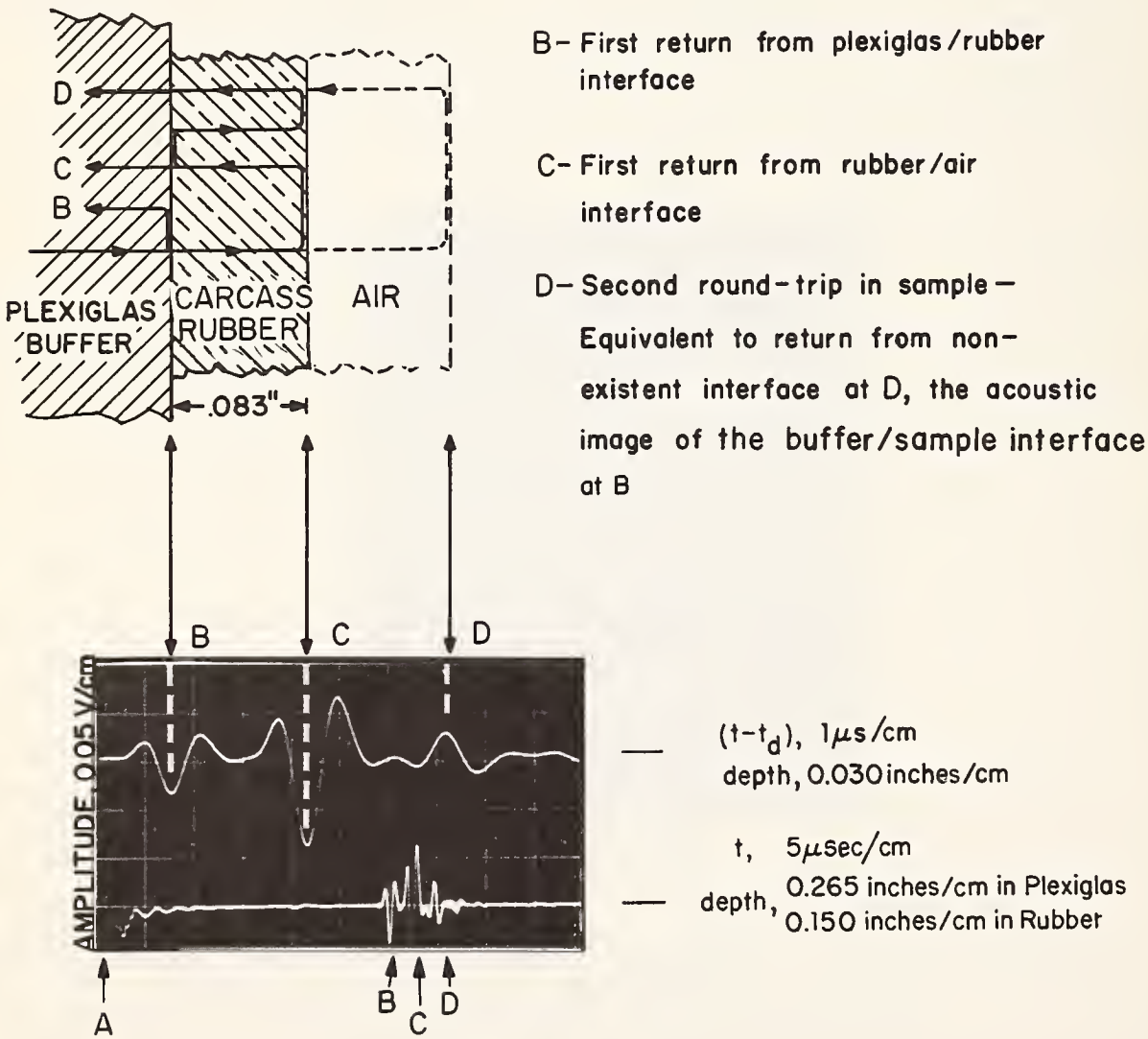

Figure 3. Reflections from Single Layer of Carcass Rubber 0.08 In. Thick (1-MHz Transducer)

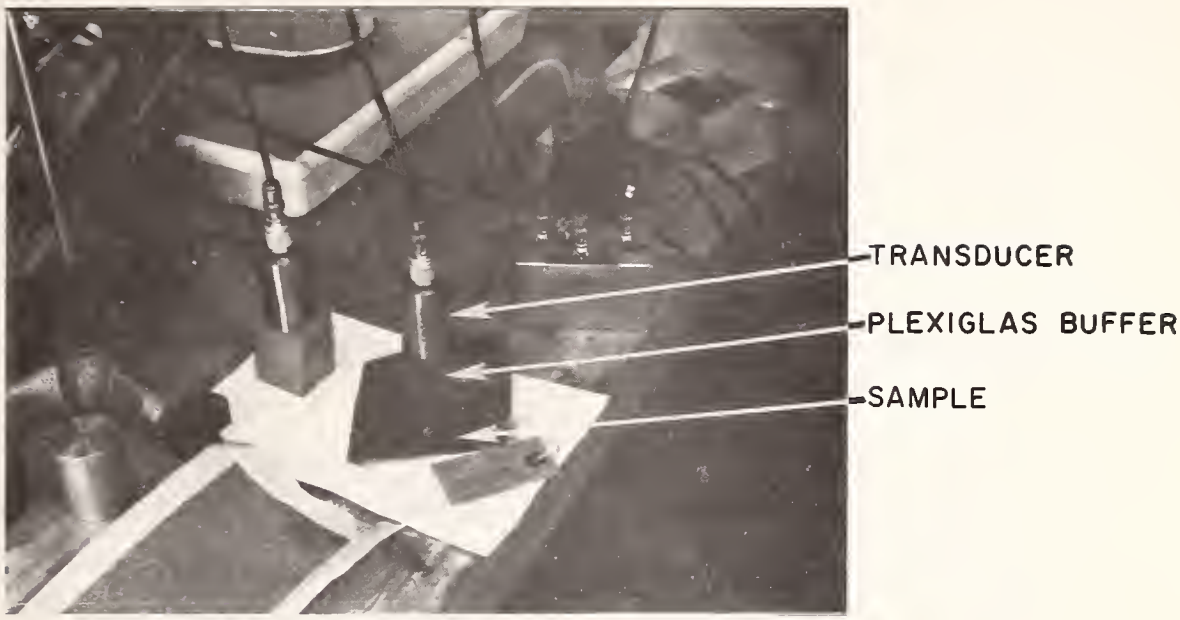

Figure 4. Contact Method for Testing Slab Specimens

reflections from the sample to be observed at a time when the receiving circuitry has fully recovered from the main bang, and the reverberations from within the transducer backing have decayed to a negligible level. In the upper trace, the reflections (B, C, D,...) from the sample are shown in more detail on an expanded time scale, using a delayed sweep to eliminate most of the 36-microsecond interval required for the pulse to travel through the buffer. The reflection at B, at the front face of the sample, occurs at the same point in time as before, since it still corresponds to the back face of the buffer, but it is now of lower amplitude, since much of the energy is now transmitted into the rubber sample. The reflection at C is from the back face of the sample, while that at D corresponds to a second round trip within the sample. The arrival time for the pulse at D is identical with that which would be observed from a single round-trip in a sample of double thickness. From an alternative point of view,

the reflection at D can be considered to occur at a fictitious interface which is an image of the front face of the sample formed by reflection at the back face.

2.2 PULSE LENGTH LIMITATIONS

The thickness resolution exhibited in figure 3 (as limited by the pulse length) is more than adequate to separate the front and back face reflections completely for the 0.83" thick sample used. However, greater or lesser resolution may be obtained in other cases, depending on a number of factors.

Fundamentally, the pulse length is inversely proportional to its bandwidth. Besides the obvious necessity of suppressing the thickness resonance of the transducer, achievement of maximum bandwidth requires optimization of the pulser/receiver/transducer coupling circuits. Modern pulser/receiver units intended for high-resolution work typically employ fast solid-state switching devices (such as avalanche transistors) giving a low output impedance to produce a fast-rise pulse across the capacitive load of the transducer. When the echo returns, the transducer acts as a capacitive source, and it is now desirable that the pulser/receiver present a fairly high impedance load so the low-frequency content of the signal will not be severely degraded.

The work reported here was done with an improvised pulse-echo system consisting of a general-purpose laboratory pulse generator, oscilloscope, and a resistive pad and simple diode clipping circuit as shown in figure 5. Since the coupling circuitry in our system was less than optimum, the data presented herein provides a generally conservative representation of the resolution obtainable.

The actual performance of the system used is indicated by the calibration pulse forms, shown in figure 6, observed at circuit points V_M, V_T, and V_R (using the reflection from a water/steel interface). For most of the work, "pulse" excitation as shown in the leftmost set of oscillograms (a, b, e, and f) was used, the rectangular drive pulse being adjusted in width to about the half-cycle period of the transducer, to maximize the peak-to-peak value

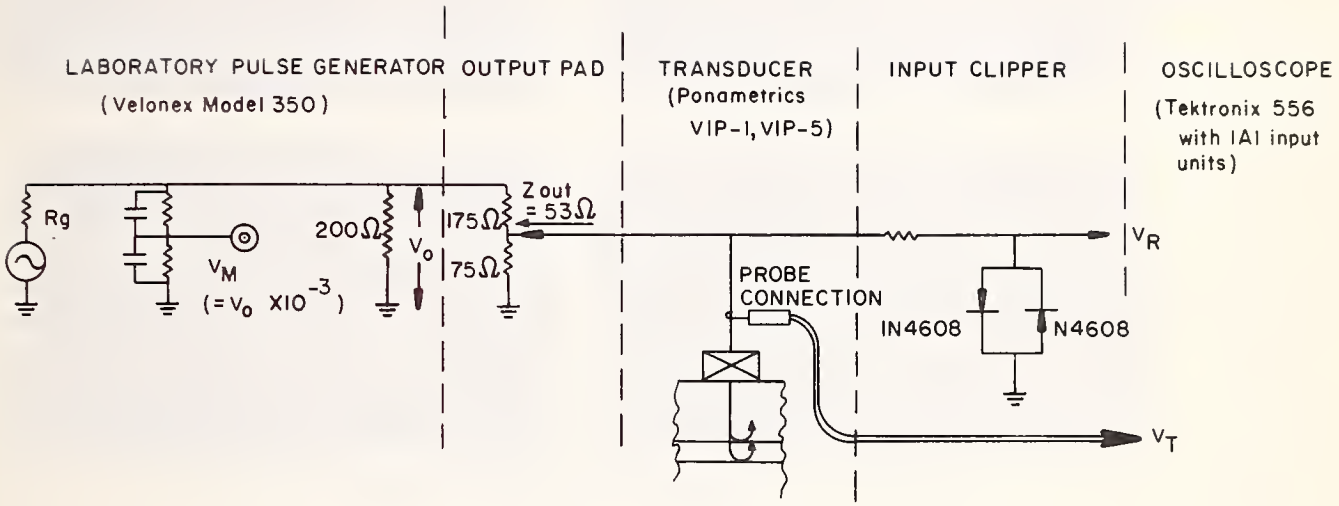

Figure 5. Pulser/Receiver Coupling Circuits

of the acoustic pulse. For some of the work with slab specimens, "step" excitation as shown in the rightmost set of oscillograms (c, d, g, and h) was employed, the rectangular pulse being made wide enough to generate separate acoustic pulses at its beginning and ending steps, spaced far enough apart that the second set of reflections does not interfere with measurement of the first set.

Under good conditions, bandwidths of 100% of the nominal frequency can be realized, and the pulse consists approximately of a single oscillation at the fundamental resonance. Reflections at two successive interfaces will then be completely resolved if the round-trip travel distance differs by a full wavelength, i.e., if the interfaces to be resolved are at least a half wavelength apart at the nominal transducer resonant frequency. Since the velocity

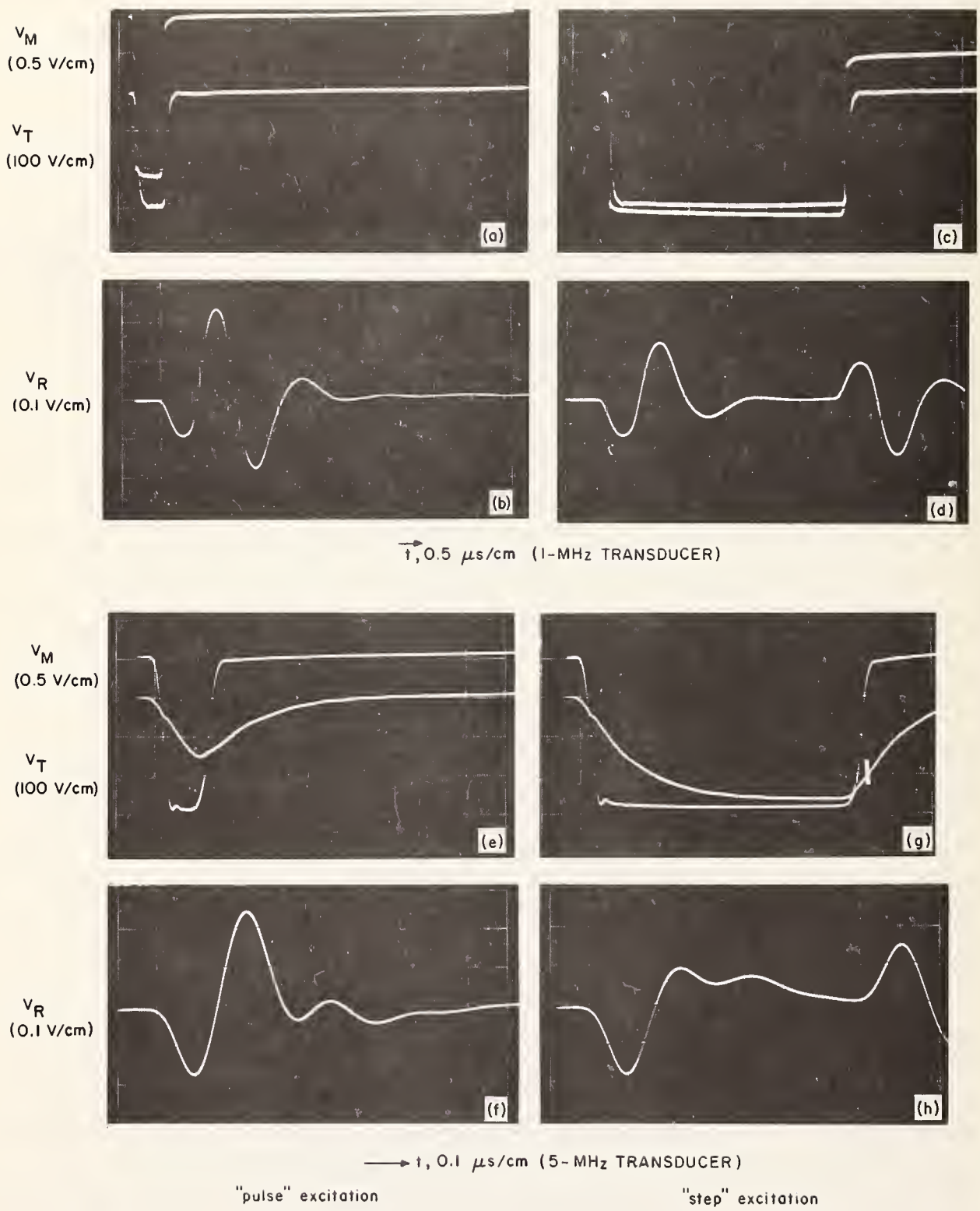

Figure 6. System Calibration Pulse Forms

of sound in tire rubbers is approximately 0.060"/microsec, this half-wavelength distance will be about 0.030" or 0.006" respectively for the 1- and 5-MHz transducers used here.

The pulse length also determines the accuracy with which a given interface can be located, i.e., the accuracy of a depth or thickness measurement. In general, the accuracy of such a measurement is much better than the half-wavelength distance corresponding to the resolution limit for adjacent interfaces discussed above. Since the shape of the pulse is known, its position in time can usually be determined to within one or two tenths of its length.

On the other hand, no matter how short the pulse may be when first radiated from the transducer, the resolution which will be realized depends on the length of the echo pulse received. Tires constitute a highly attenuating inhomogeneous medium, in which the higher frequency components of the pulse spectrum are more strongly absorbed and scattered. Therefore, for echo pulses received from deeper layers within a tire, the pulse spectrum is progressively narrowed, and the pulse length is correspondingly increased, degrading the depth resolution obtainable. This factor introduces a principle of diminishing returns as one endeavors to improve the resolution by raising the basic frequency of the transducer. The bandwidth of the pulse is also degraded by beam-spreading losses, which most severely degrade the low-frequency content of the pulse, since a transducer of given size is less directional at low freqeencies.[7] As we shall see, in typical tire structures, the degraded pulse returned from maximum depth can be as long as 3.5 microseconds, corresponding to a spacing of about 0.1" between resolvable interfaces. However, an anomaly can be detected even if its reflection signal is not completely resolved from other reflections. It is merely necessary that the disturbance to the normally present reflection signal be observable, either as a change in amplitude, or perhaps as an apparent shift in the time position of a pre-existing reflection signal.

3. REFLECTIONS AT INTERFACES

We have seen that with highly damped transducers having nominal resonant frequencies in the 1- to 5-MHz range, ultrasonic pulses are available which are short enough to provide useful resolution of the laminar structure of a tire. Before proceeding to an examination of the reflection signals actually obtained, it will be helpful to look briefly at the dependence of interface reflections on the properties of the materials forming the interface. These phenomena are discussed at length in the standard handbooks on ultrasonic testing[8,9] and derivations of the cited equations are presented in elementary texts.[11]

3.1 INTERFACE BETWEEN TWO MEDIA

When sound in medium 1 is incident normally at a boundary with medium 2, the fraction of energy reflected is given by

$$R_{1,2} = \left(\frac{Z_2 - Z_1}{Z_2 + Z_1}\right)^2 = \left(\frac{Z_2/Z_1 - 1}{Z_2/Z_1 + 1}\right)^2 = \left(\frac{r-1}{r+1}\right)^2 \qquad (3\text{-}1)$$

while the fraction transmitted is

$$T_{1,2} = \frac{4Z_1Z_2}{(Z_2+Z_1)^2} = \frac{4(Z_2/Z_1)}{(Z_2/Z_1 + 1)^2} = \frac{4r}{(r+1)^2} \qquad (3\text{-}2)$$

in which Z_1 and Z_2 are the acoustic impedances of the initial and final media, and we have defined $r = Z_2/Z_1$ as the impedance of the second medium relative to the first.

The acoustic impedance (or more properly, the "specific acoustic impedance") is a characteristic property of any material, quantitatively given by the product of its density and the velocity of sound in that material, i.e., $Z = \rho V$. But the velocity of sound is $V = \sqrt{B/P}$, where B is the bulk modulus of elasticity (for the longitudinal waves considered here). Thus, acoustic

impedance is given by

$$Z = \rho V = \rho\sqrt{B/\rho} = \sqrt{\rho B}. \qquad (3\text{-}3)$$

Physically, the bulk modulus defines the resistance of a material to compression, by giving the compressive stress, i.e., the increase in pressure (ΔP) required to produce a small fractional reduction in volume ($-\Delta V/V$):

$$B \doteq \text{Bulk modulus} \doteq \frac{\text{stress}}{\text{strain}} = \frac{\Delta P}{\left(-\frac{\Delta V}{V}\right)} \qquad (3\text{-}4)$$

Thus, materials which are hard and/or heavy have high values of acoustic impedance, whereas easily compressible, low-density materials have low impedance. Some representative values of acoustic impendance for materials which will be of interest are given in Table 3-1.

TABLE 3-1. VALUES OF ACOUSTIC IMPEDANCE

Material	Acoustic Impedance $Kg/(m^2 \cdot sec)$	Ref	Impedance Ratio to Water
Air	0.000415×10^6	11	2.8×10^{-4}
Water	1.48×10^6	12	1.0
Ethanol	0.9535×10^6	10*	0.644
Ethylene Glycol	1.8454×10^6	10*	1.248
Carcass Rubber	1.66×10^6	**	1.12
Tread Rubber	1.84×10^6	**	1.24
Nylon	$2.0\text{-}2.7 \times 10^6$	12	1.35 to 1.82
Teflon	3.0×10^6	12	2.03
Quartz, fused	14.5×10^6	12	9.8
Lead Metaniobate	16.0×10^6	12	10.8
Aluminum	17.3×10^6	12	11.7
Steel	46.7×10^6	12	31.5

*Values for ethanol and ethylene glycol are calculated from density and velocity data given by Weant, R.C., ed., Handbook of Chemistry and Physics, 49th Ed., Chem. Rub., Cleveland, Ohio (1968), p. E-38

**Values for carcass rubber and tread rubber were measured by comparing reflection amplitudes in water with those for known materials, as explained in the appendix.

The transmission and reflection coefficient values calculated for impedance ratios from 1:10 to 10:1 are plotted in figure 7. It is evident that water provides a very good impedance match to tire rubbers, the energy reflection coefficient being 1% or less. It is equally clear that air would provide an intolerably poor medium for coupling energy from a thickness-mode piezoelectric transducer. For a lead metaniobate transducer, the impedance ratio to air is $Z_2/Z_1 = (0.000415 \times 10^6)/(16 \times 10^6) = 2.56 \times 10^{-5}$, and the transmission coefficient calculated from Equation 3-2 is 1.03×10^{-4}. Similarly, the calculated energy transmission factor from air to tread rubber is 8.8×10^{-4}. For the two-way path, the energy returned would be down by 14 orders of magnitude!

It is evident that reflections between the various kinds of rubber in tires will be very small, probably much less than 1% in the cases of most interest. However, the smallness of the reflection is no cause for despair, since currently available pulser/receiver units operating even with highly-damped transducers can detect reflections representing a return of only one part in 10^{10} of the outgoing energy.[13]

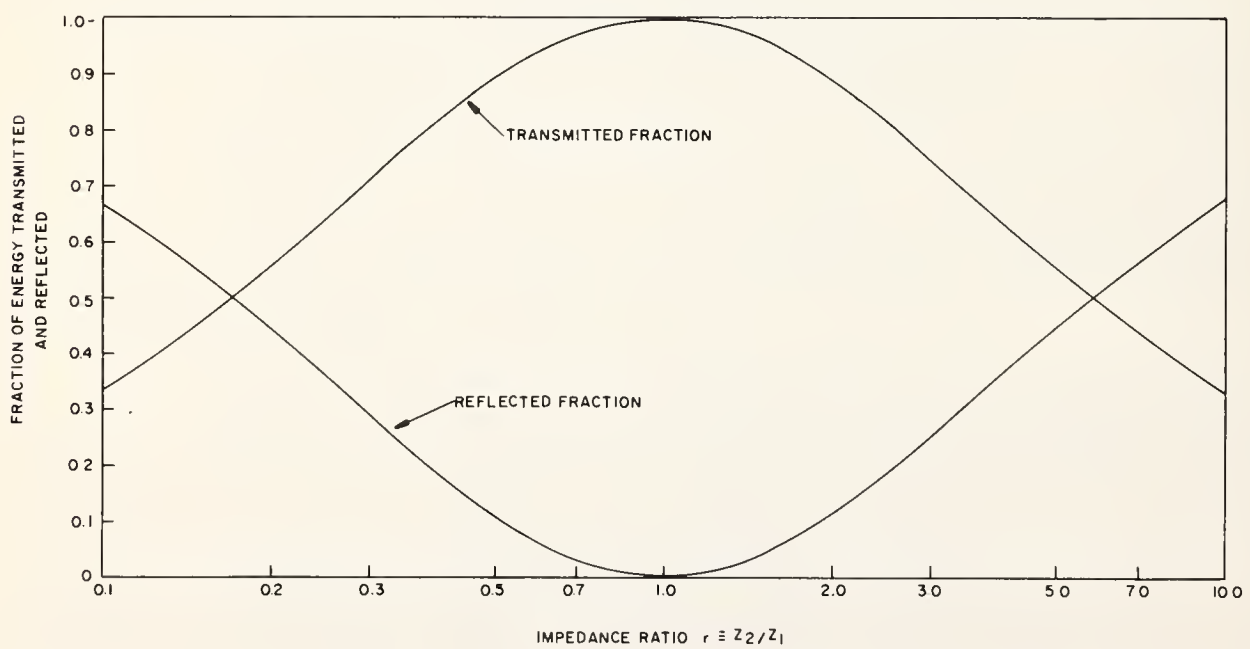

Figure 7. Reflection and Transmission Coefficients for a Simple Interface between Two Media

Furthermore (as was mentioned earlier), it is precisely because the reflection coefficient is so small to begin with that an overwhelming advantage lies with reflection measurements for observing small variations in materials properties in the vicinity of an interface. The amplitude reflection coefficient is given by

$$R = \frac{Z_2 - Z_1}{Z_2 + Z_1} \qquad (3\text{-}5)$$

and in the case where the difference in impedances $\Delta Z \equiv Z_2 - Z_1$ is small, $Z_1 \cong Z_2 \equiv Z$, and we have approximately

$$R \cong \frac{\Delta Z}{2Z} . \qquad (3\text{-}6)$$

Thus, the reflected pulse amplitude is directly proportional to the fractional change in impedance across the interface. The smaller ΔZ, the smaller will be the percentage change in Z_1 or Z_2 that will correspond to a given percentage variation in the reflection amplitude.

3.2 THIN INTERMEDIATE LAYERS

The discussion thus far applies strictly to isolated interfaces, but in practice it will remain valid provided that the reflection pulses from nearby interfaces do not overlap significantly. If two interfaces are separated by a distance less than the pulse length, the individual reflections will interfere with each other, and the overall reflection and transmission characteristics of the double interface will depend not only upon the acoustic impedances of the three media, but also on the thickness of the intermediate layer in relation to the wavelength in that medium. Such a system is a useful model for a separation, and for the liquid film customarily used to augment contact coupling. It is also useful as a first approximation to conditions existing at a poorly-bonded interface.

An exact solution to the problem of transmission of single-frequency sound through two interfaces separating three media of acoustic impedances Z_1, Z_2 and Z_3 is derived by Kinsler & Frey.[11]

Defining the impedances of the final and intermediate layers relative to the first as $r = Z_3/Z_1$ and $r' = Z_2/Z_1$, their result can be written

$$T = \frac{4r}{(r+1)^2 \cos^2(k'\ell) + \left(r' + \frac{r}{r'}\right)^2 \sin^2(k'\ell)} \qquad (3\text{-}7)$$

where ℓ is the thickness of the intermediate layer. and $k' = \frac{2\pi}{\lambda_2} = \frac{2\pi f}{V_2}$ is the wave number in that layer, where the velocity is V_2 and the wavelength is λ_2.

In the case of a separation occurring at the bond between two rubber compounds (such as tread rubber and carcass rubber), the initial and final impedances differ little, and $r \tilde{=} 1$. We may presume that the disbonded surfaces are essentially in contact, i.e., that ℓ is small compared to the wavelength. In this case, $\sin^2(k'\ell) \tilde{=} 0$ and $\cos^2(k'\ell) \tilde{=} 1$, and one might at first expect that the $\sin^2(k'\ell)$ term could be neglected, in which case the expression would reduce to

$$T \tilde{=} \frac{4r}{(r+1)^2} = \frac{4r}{(2)^2} \tilde{=} r \tilde{=} 1. \qquad (3\text{-}8)$$

However, if the intermediate layer is of grossly different impedance, the $\sin^2(k'\ell)$ term does <u>not</u> become negligible merely because $\ell << \lambda_2$, since it is multiplied by the factor $(r'+r/r')^2$. This factor is very large if r' is either very large or very small.

Figure 8 shows the overall transmission calculated from Equation (3-7) for 1-MHz ultrasound as a function of the intermediate layer thickness, for several intermediate materials interposed between tread and carcass rubber (r = 0.9073). It is seen that if the intermediate material is air, the separation will be essentially opaque acoustically if the rubber surfaces are separated by only ten millionths of an inch! The magnitude of this result justifies the initial assumption that the separation is gas filled, since even if the surfaces are in dry "contact," practical surfaces are rough on such a microscopic scale, and

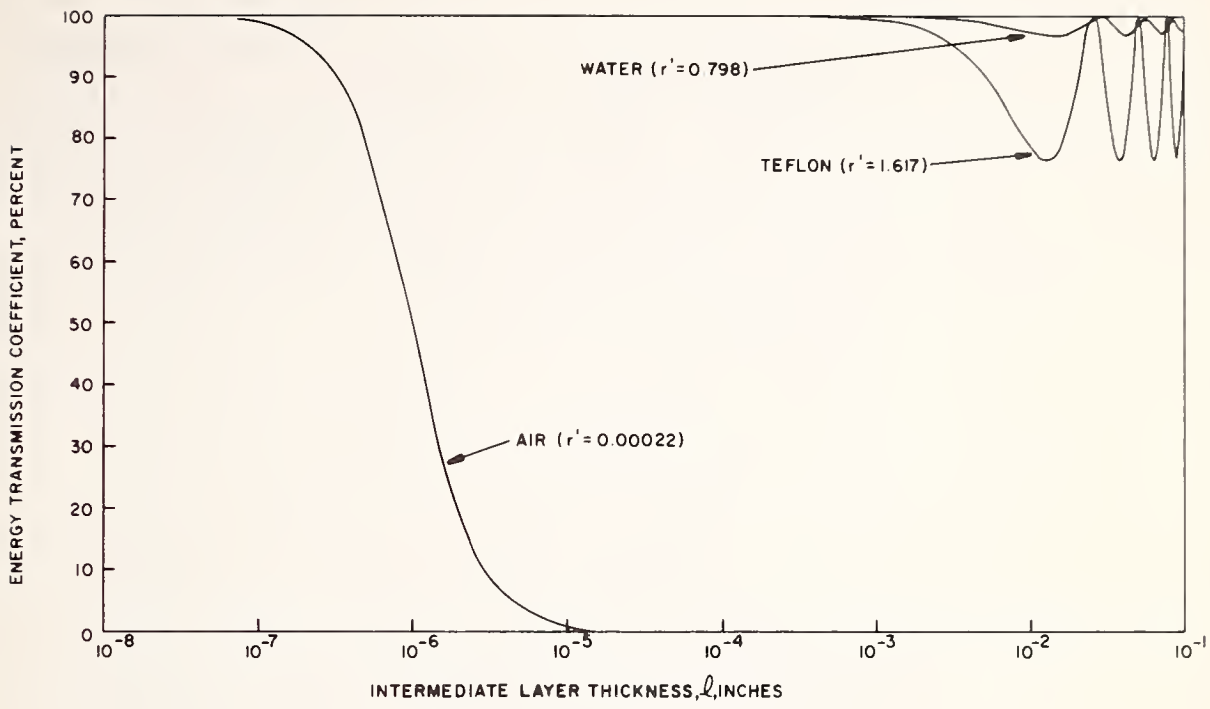

Figure 8. Transmission of 1-MHz Ultrasound through a Thin Intermediate Layer between Tread and Carcass Rubber Stock

really touch only at scattered high points representing only a small percentage of their area. The curves for Teflon and for water show that if the impedance of the intermediate material is at all comparable to that of the rubber, the transmission is very near 100% so long as the intermediate layer is thin compared to the wavelength. For thicker intermediate layers, maxima and minima of transmission occur as the layer thickness passes through multiples of $(\lambda_2/4)$, the maximum values of reflection remaining small if the disparity in impedance is not large.

The pulses employed in high resolution work are not single-frequency waves, but have a broad frequency spectrum, and the preceding discussion must be considered as it applies to various portions of the spectral content. If the prediction is for near total reflection or near total transmission for all frequencies of significance, the entire pulse is reflected or transmitted as the case may be. In intermediate cases, the pulse reflection

becomes frequency-selective, and spectral analysis of the reflected pulse can provide a powerful method for determining various characteristics of the thin reflecting layer.[7] According to Equation 3-7, a transmission maximum should occur for an air-filled separation which is half-wave resonant. Such a maximum has been omitted from the curve in figure 8, since such a resonance would be very sharply tuned, and of little consequence for short-pulse ultrasound, since its pass band would accept only a negligible fraction of the energy in the pulse spectrum.

4. REFLECTION SIGNALS FROM REPRESENTATIVE TIRE STRUCTURES

This section discusses the examination of the acoustic reflection signals obtained from representative tire structures. On the one hand, data will be presented on slab specimens made from actual tire component materials cured together in a laboratory press, usually with various deliberately introduced or programmed defects. Data on such samples serve to exhibit the acoustic signatures characteristic of particular laminar structures and various defects observed under ideal conditions. On the other hand, we will examine reflection signals obtained in small sections cut from actual tires, to see the nature of the reflections due to the internal structure normally present. Such reflections constitute the background clutter against which the characteristic signatures of various anomalies must be detected. Data on samples cut from actual tires also provide a basis for estimating the allowances which must be made for degradation of characteristic defect signatures because of loss of signal strength and loss of time-resolution due to propagation through the tire materials.

4.1 METHODS FOR A-SCAN MEASUREMENTS

Here, we will examine various individual reflection signals taken one spot at a time. The oscilloscope display of such a reflection signal, giving echo amplitude as a function of time (or, equivalently, as a function of depth into the sample) is conventionally called an A-scan presentation, even though no actual mechanical scanning of the transducer relative to the test object is involved. The reflection signal obtained at various points on a slab sample can be examined using the buffered contact technique as illustrated in figure 4, and similar comparisons can be made on a cut section of a tire immersed in water in a tray as shown in figure 9.

More reproducible results are obtained on slab specimens by employing the "bottomless bucket" apparatus shown in figure 10. Here the slab sample to be tested is laid flat on a cork-surfaced

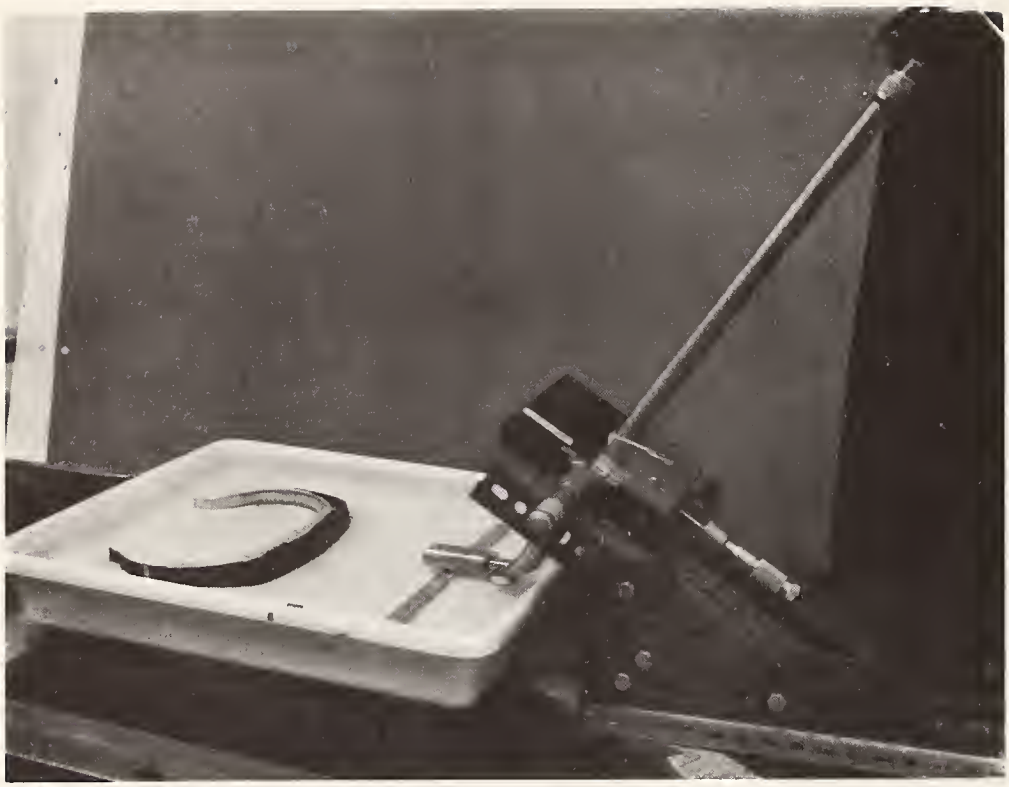

Figure 9. Tray Immersion Setup for Tire Sections

board and a cylindrical ring is clamped down upon it to form a cylindrical tank closed at the bottom by the sample itself. The tank is filled with water for acoustic coupling to the top face of the sample. The cork surface below the sample provides a near zero acoustic impedance insuring an essentially total reflection at this point. The transducer is dipped into the surface of the liquid, at the open top of the bucket, where it is supported independently by rod and clamp hardware attached to the bench top. The entire bucket assembly was later adapted to produce the one-dimensional scanning displays presented in the next paragraph, by placing rollers between the base board and the bench top, and adding a single-axis motorized lead screw drive.

The size of the spot characterized by a single A-scan reflection signal corresponds to the cross section of the acoustic beam. Except for figure 21(a), to be discussed later, all data presented here were taken with plane wave; i.e., (unfocused) transducers having nominal resonant frequencies of

Figure 10. Bottomless Bucket Immersion Tank for Slab Specimens

one or five MHz, with active face diameters of 1" and 3/4" respectively. Data were taken at test distances well within the near field distances ($N = \frac{D^2}{4\lambda}$, where λ is measured in water) which are 4.25" and 12.0" respectively. Within this range the radiation field from such transducers is approximately a collimated beam having a cross section diameter equal to that of the active face. Thus the size of the surface resolution element is approximately 1" or 3/4" for the 1-MHz and 5-MHz data respectively.

For detecting small flaws it is generally recommended that the test distance be kept equal to or larger than the near-field distance, since marked amplitude variations due to interference effects within the near field lead to unpredictable echoes for small flaws. For work of the type discussed here, however, this consideration appears to be relatively unimportant - for several reasons. In the first place, we are concerned with laminar structures subject to laminar defects large enough to average out amplitude variations over the beam cross section. Furthermore, near-field interference effects are much less severe for broad-band short pulses because of frequency averaging.[7] For whatever reasons, it has been verified experimentally that results are remarkably insensitive to test distance for a variety of laminar structures and programmed defects.

4.2 SEPARATION AND POROSITY IN TWO-PLY SLAB

Figure 11 shows spot-to-spot comparison measurements made using the buffered-contact procedure on a slab specimen. This sample consists of two layers of ply fabric with outer covering layers of plain rubber ("skim stock"). A separation between the ply layers was deliberately introduced by pre-curing a 1"-diameter spot and applying a spot of stopcock grease prior to the final overall cure in the laboratory press. The signal at corner 1 shows the sort of reflection signal normally expected, with clear reflections at the front and back faces, and lesser reflections in between, attributable to the ply fabric. In the center, the reflection due to the separation is seen at 3.2 microseconds, and the former back reflection at 5 microseconds is essentially gone, since the acoustic energy is almost totally reflected at the separation. Clearly, the separation could have been detected by gating out the portion of the signal between the front and back reflections, say, between 2 and 4.5 microseconds, and then applying a detection threshold somewhat above the ply reflection amplitude.

Corners 2 and 3 show a greatly attenuated back reflection without the presence of the reflection from the separation. This combination of results indicates excessive attenuation in the

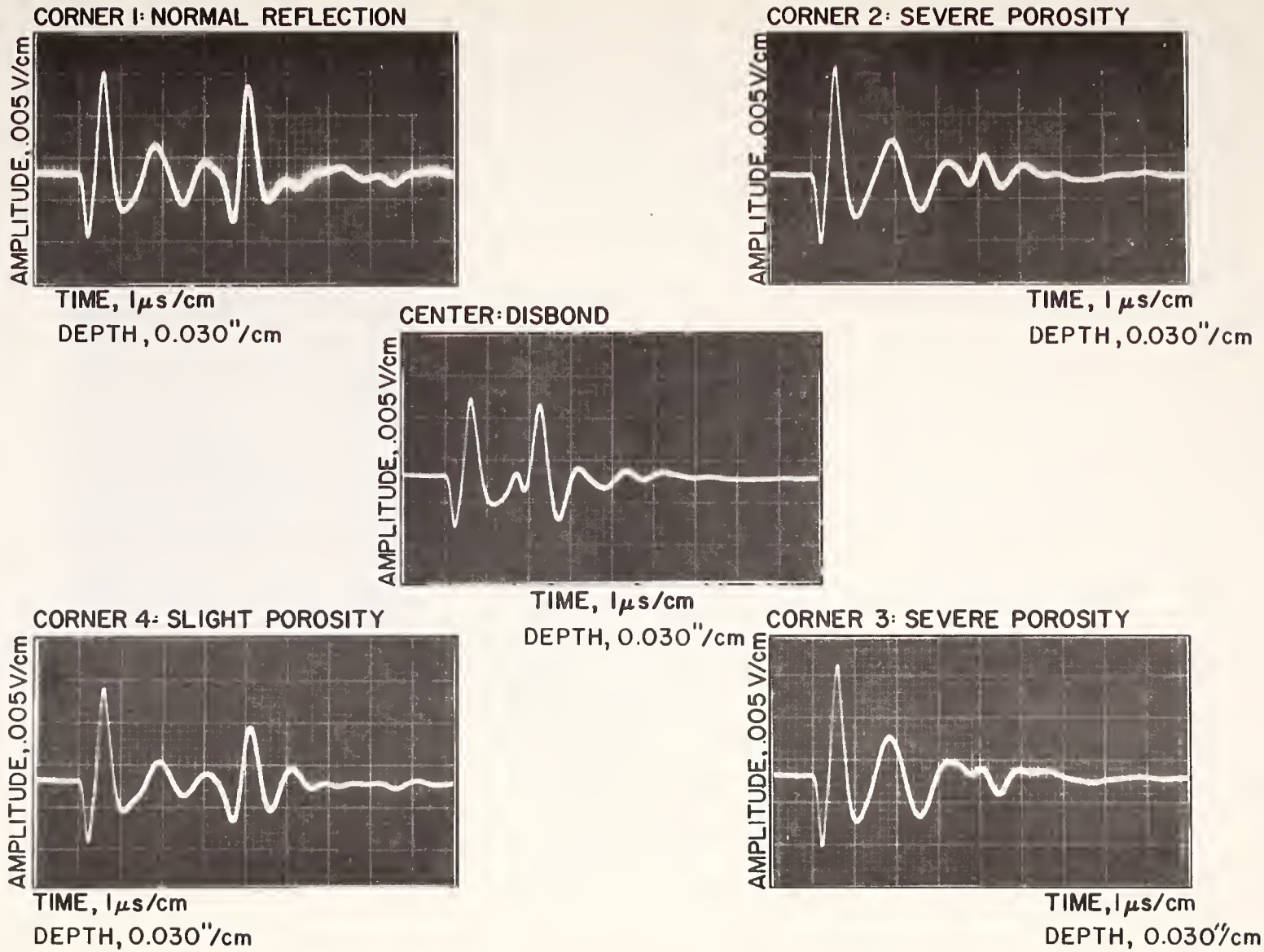

Figure 11. Separation and Porosity in a Slab Sample (Contact Technique, Using 5-MHz Transducer and 2-inch Plexiglas Buffer)

rubber attributed in this case to porosity. (This was a preliminary sample, cured between flat plates, and flow of the rubber caused inadequate molding pressure at the edges.)

4.3 INTERFACE BETWEEN TREAD AND CARCASS RUBBERS

A demonstration that the interface between tread rubber and carcass rubber is detectable is given by figure 12, which shows the details of the reflections near the back surface of a tread-rubber/carcass-rubber sample. These data were taken using water-coupling in the "bottomless bucket" apparatus (figure 10). The front surface reflection is not seen because of the delayed sweep. The largest pulse is, of course, the return from the back surface (rubber/cork interface), while the smaller pulse to the left is the reflection from the tread/carcass interface. The similar reflection occurring after the back-surface reflection is the reverberation between the tread/carcass interface and the back surface, corresponding to ray-path D in Figure 3. Using methods explained in the appendix, it can be calculated that the

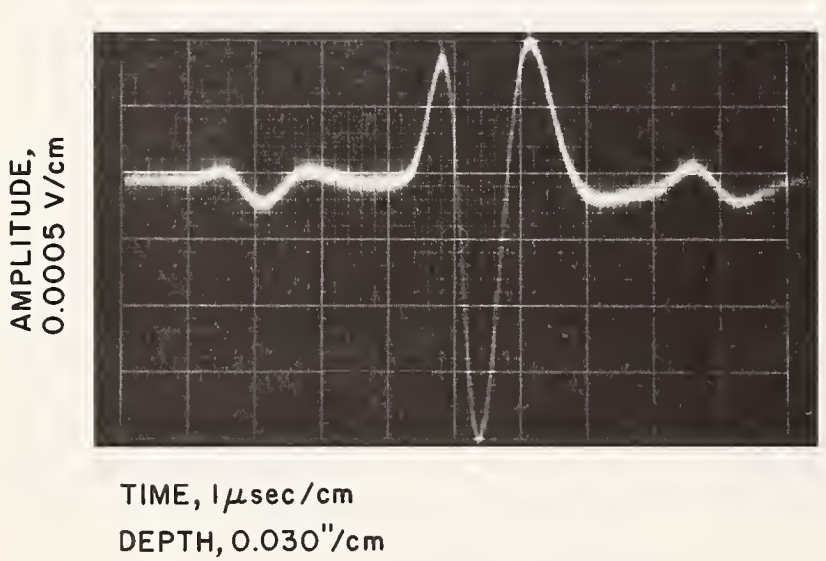

Figure 12. Reflection at Tread Rubber/Carcass Rubber Interface between Tread and Carcass Rubber (5-MHz Transducer)

energy reflection coefficient at the tread/carcass interface is 0.2% (-27 db), corresponding to an acoustic impedance difference between the two media of about 10%. This data represents a worst-case condition, since it is obtained at five MHz, where the signal suffers also from a 38 db attenuation loss in the round trip through the tread rubber, so the total return is down some 65 db with respect to the incident sound pulse. There is still a generous signal-to-noise ratio even though the circuitry is less than optimum, as discussed previously. A well-optimized pulser/receiver would have about 20 dB better signal/noise ratio.

4.4 TIRE SECTIONS

We now turn to some representative reflection signals obtained on sections sliced from actual tires, examined using water coupling in the stationary immersion setup (figure 9). Here the tire section is placed in a tray of water, with a wetting agent added, and the transducer is mounted with an adjustable elbow fitting on the end of a section of waterproof solid coaxial line commonly called a "search tube." An X-Y manipulator at the outer end of the search tube permits precise aiming of the transducer so its axis is normal to the reflecting surface of interest in the tire. The cut surfaces of the tire section are coated with "Silastic" silicone rubber to prevent water penetration of the exposed cord ends, which would alter their acoustic properties. To provide a medium with very low acoustic impedance on the inside of the tire to simulate the internal air volume in an inflated tire, a layer of foam insulating tape was applied to the inner surface, and waterproofed with the "Silastic" compound.

Figure 13 shows oscillograms of the reflection signals obtained with 1- and 5-MHz transducers, correlated with the internal structure in the tread region of a double-belted radial tire. The sound pulse is incident from the left, and the echoes on the extreme right, from the carcass/air interface at the inside of the tire, show that a useful degree of resolution is still obtained with frequencies low enough to penetrate all the way through this 6-ply structure. This result is fundamental because

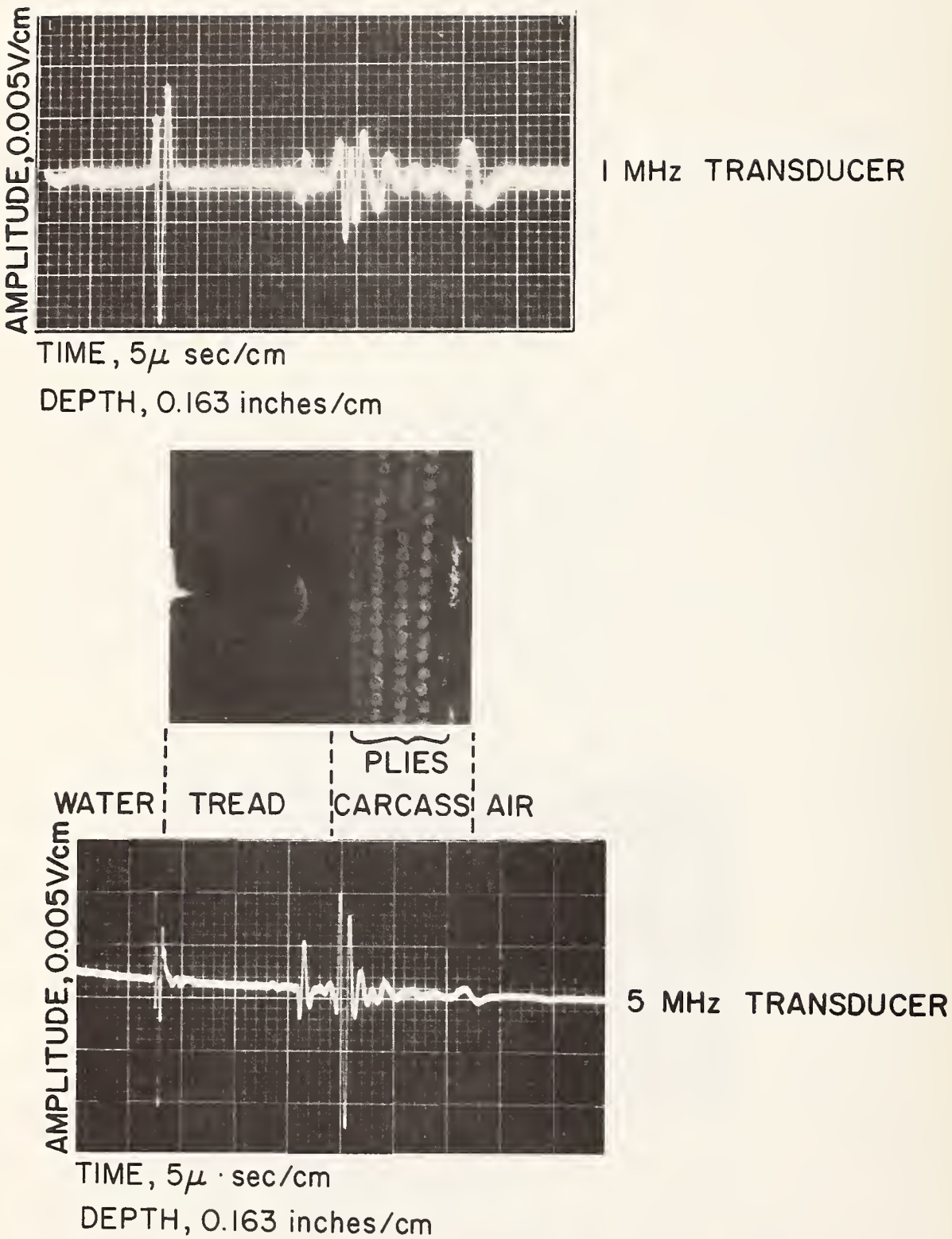

Figure 13. Reflection Signal Matched to Structure in the Tread Region of a Double-Belted Tire

penetration and resolution stand in a trade-off relationship depending on the choice of transducer frequency. Resolution can be improved by using the shorter pulses obtainable from higher frequency transducers, but penetration will be degraded since the attenuation in rubber increases with frequency. Thus, these oscillograms alone prove that a feasible compromise is available, and show in fact that the optimum frequency is in the range of 1 to 5 MHz, depending on the relative importance attached to penetration vs. resolution.

The front surface reflection (at the water/tread interface) shows a fairly clean return at 1-MHz, whereas 5-MHz this return shows a more complicated structure indicating surface irregularities which were not resolved by the 1-MHz pulse. The oscillatory response in the latter half of the signal is a composite of the reflections from the six ply layers, which in this instance are not individually resolved. The sharply isolated reflection just ahead of the ply reflections (at 25 microseconds on the time scale for the upper oscillogram) comes from the water/rubber interface at the bottom of the tread groove.

The back surface (carcass/air) reflection is of much lower amplitude for the 5-MHz transducer than for the 1-MHz, showing the effects of frequency-dependent attenuation and reflection losses in the composite structure. At either frequency these reflections appear much broader than the corresponding front surface reflections. In part this broadening results from the fact that the higher frequencies contained in these broadband pulses are more severely attenuated in the rubber. Since the reflection coefficient at a simple interface between two media is independent of frequency, the nearly-equal front surface reflections tell us that the incident amplitudes were about the same. Thus, the larger reflection from the first ply obtained with the 5-MHz transducer indicates a greater reflection coefficient. Normally, a greater reflection coefficient would imply a larger change in acoustic impedance. Now, the acoustic impedances of the rubber and cord fiber materials themselves do not vary to this degree. Rather, the 1-MHz frequency tends to be governed by the average properties of the composite, since its .063"-wavelength is somewhat larger than the cord dimension, while the 5-MHz frequency, having a 0.012"-wavelength,

tends to respond directly to the larger impedance discontinuity between rubber and cord. As a result, the first ply layers encountered take out most of the higher-frequency content of the 5-MHz pulse, leaving the lower-frequency components of the pulse spectrum to penetrate to the full depth of the tire. If we compare the back-surface reflections (at the carcass/air interface), we see that the pulse length is about 3.5 microseconds in either case. The 5-MHz transducer delivers considerably greater resolution and signal strength in the outermost layers, but in the de deeper regions the resolution is not much better than with the 1-MHz transducer and the signal strength is lower.

Thus, transducer frequencies generally in the range of 1 to 5 MHz are suitable for tire testing. The choice within this range is not critical, since short pulses have a broad spectral content. The echo return contains all frequencies within the incident pulse spectrum up to the highest frequencies effectively propagated through the medium under investigation.

At 5 MHz, the signal-to-noise ratio in the deeper regions is quite adequate, as is demonstrated in figure 14, which shows the 5-MHz reflection enhanced by TVG (Time-Varied Gain, also known as DAC, for Distance Amplitude Correction) in the receiver circuit, to compensate for the greater attenuation of the echoes from the deeper regions. With TVG it is comforting to note that the total reflection at the inner surface of the tire does exceed the reflections from the adjacent ply layers, indicating the separations throughout the tire could be discriminated from the ply reflections solely on the basis of amplitude, provided that suitable TVG is applied first.

By pulsing the gain variation circuit, the receiver can be gated to select a particular isolated reflection as shown in figure 15. The gated signal made so available is a repetitive pulse which can be peak-rectified and used as the input variable for various scanning type displays. (Adjustable time-varied gain and variable-width signal gates timed either from the initial pulse or from an earlier reflection are standard features of many commercial ultrasonic instruments.)

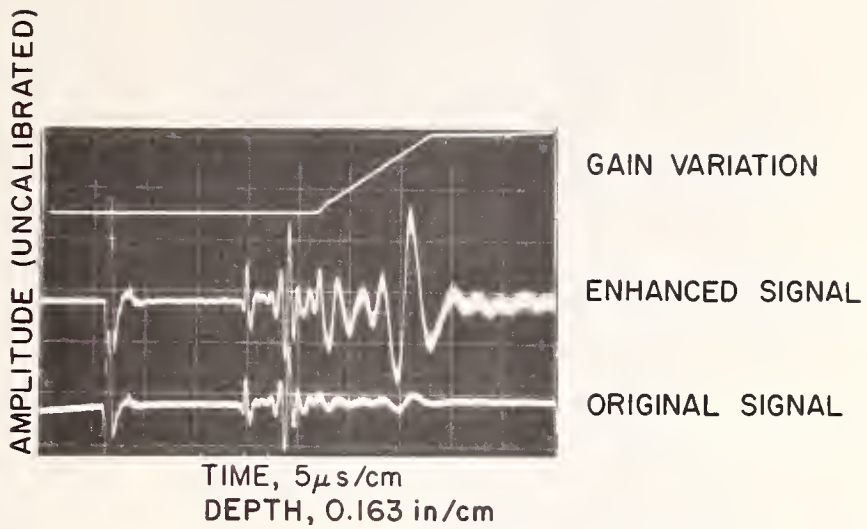

Figure 14. Time-Varied Gain Enhancement of Reflection Signal (5-MHz Transducer)

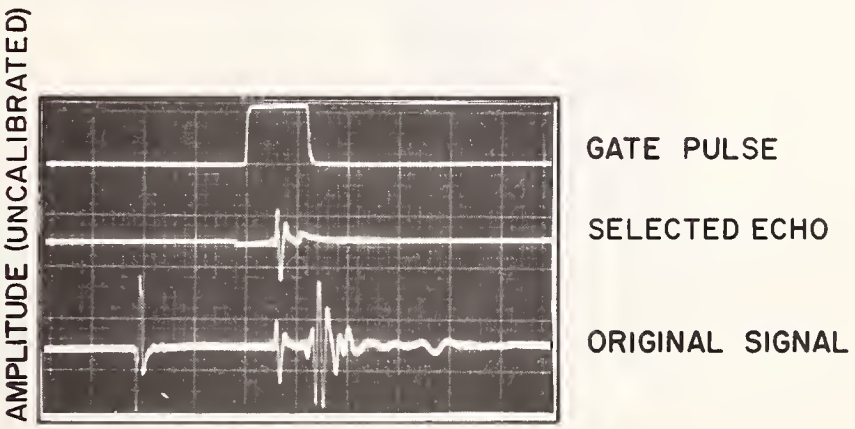

Figure 15. Gate Selection of an Echo Signal (5-MHz Transducer)

Figures 16 and 17 show the alterations in the reflection signal corresponding to various other regions of the tire. The time separation between reflections varies directly with the thickness of the components involved, and reflection amplitudes change both on an absolute basis and relative to each other. At the sidewall (figure 16), the first ply reflection is larger, because there is less rubber to attenuate the signal, and the front surface reflection (the water/rubber interface) is reduced because the

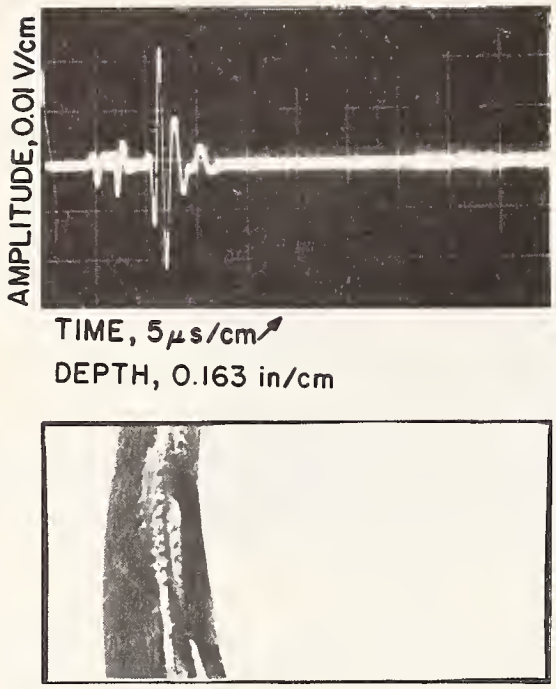

Figure 16. Reflection Signal Matched to Sidewall Structure (1-MHz Transducer)

the axis of the transducer has been aligned normal to a plane tangent to the ply layer, to maximize the ply reflection. Since the thickness of the cladding rubber varies around the cross section, the outer surface of the tire exhibits a wedge angle with respect to the ply, and is not simultaneously normal to the axis of the transducer. Wave fronts returning from the outer surface are thus titled with respect to the surface of the transducer, and do not arrive in phase, i.e. at the same time, over all points on the surface of the transducer. In figure 17, for the shoulder region, reflection amplitudes are down some 20 db compared to the tread region. The loss in amplitude is due in part to the fact that the reflecting surfaces are more strongly curved in the shoulder, leading to curvature of the reflected wave fronts, which then do not arrive in phase over the surface of the transducer. The outer surface reflection becomes ragged in character, since it consists of a multiplicity of small echoes scattered from surface relief features at varying distances. However, the specular glint from the nearest part of the surface is sharp enough to serve as a time reference mark for thickness measurements or echo gating.

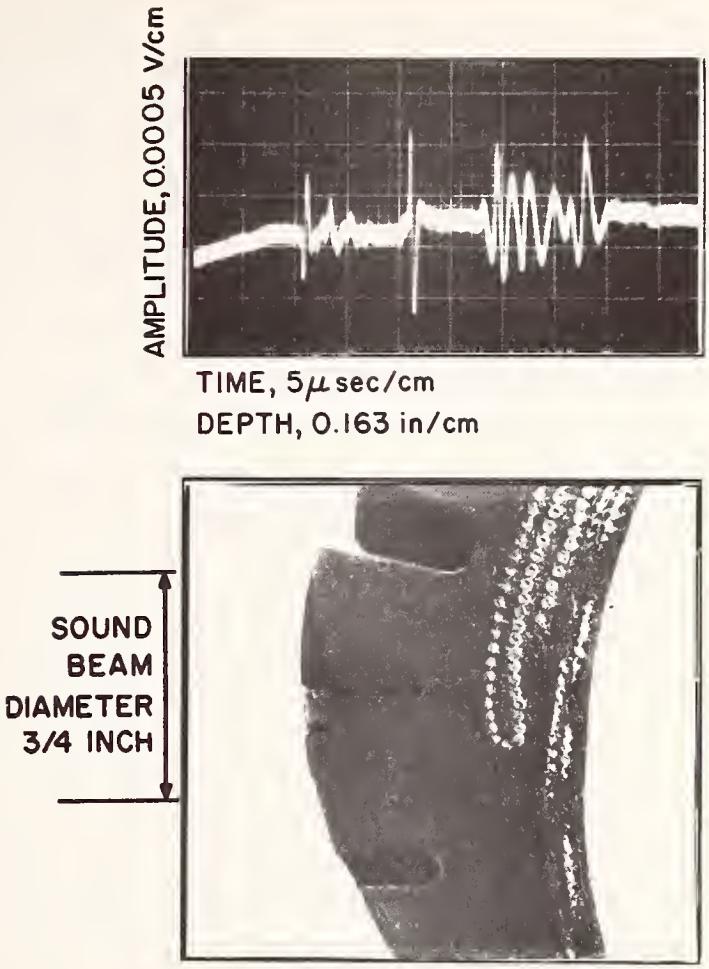

Figure 17. Reflection Signal Matched to Shoulder Structure (5-MHz Transducer)

5. SCAN-GENERATED DISPLAYS

On the one hand, the spot-to-spot comparisons which have been presented demonstrate the wealth of information which can be derived from detailed analysis of reflection signals. As explained in the appendix, quantitative analysis of such data will yield quantitative results for acoustic impedances, acoustic velocities, attenuations, reflection coefficients, etc. On the other hand, the exercise illustrates the tedious and time-consuming nature of the process. When searching the large surface areas encountered in tire testing, automatic scanning methods become an economic necessity. We shall see that when variations in the reflection signals are subtle, the use of image-type displays synchronized to mechanical scanning of the object is not just a luxury, but is essential to recognition and interpretation of the variations.

5.1 SCANNING DISPLAY TECHNIQUES

It is conventional in ultrasonic testing to refer to the mode of data acquisition and the resulting display as an A-, B-, or C-scans. The classification is made according to the number of dimensions (in "degrees of freedom") involved in mechanical scanning. That is to say, an "A-scan" actually involves no mechanical scanning, but refers to the oscilloscope presentation of echo amplitude versus round-trip travel time, or depth into the specimen, which is observable at a single location. A "B-scan" involves the relative motion of the transducer along a one-dimensional path on the surface of the tested object. In a "C-scan," a surface of the object inspected is systematically covered by a two-dimensional scan.

B-scan and C-scan inspections ordinarily generate image-type data displays. A C-scan recording is usually made by synchronizing the line scan and chart paper motions of a facsimile type recorder to the two mechanical scanning coordinates. As the surface of the tested object is systematically covered by the mechanical scan, the echo amplitude occurring within a suitably timed signal gate modulates the printing density of the facsimile recorder to produce a

photograph-like image which maps the surface scanned. For a B-scan, one axis of the image display corresponds to the distance measured along the one-dimensional scanning path, but the other axis still corresponds to the pulse travel time, and hence measures the depth from which echoes have been returned. The image display thus corresponds to a cross-section picture of the test object as it would appear sliced vertically along the scan path.

C-scan recording provides a very readily interpreted display, but would involve special difficulties for tires. For objects having simple external shape and homogeneous internal composition, it is only necessary to establish a signal gate which excludes the front surface and back surface reflections, and to modulate the printing density according to the amplitude of the signals received within this gate. Dark (or light) printed areas on the C-scan image then indicate the presence of flaws, and show their location, severity, size, and shape in a pictorial way. In the case of tires, such techniques would be applicable for mapping the locations of gross defects such as separations. Since separations lying deep in the tire structure will not generally produce reflection signals as large as the reflections from the outermost plies, it will be necessary to apply a suitably programmed T.V.G. (Time Varied Gain), to utilize the fact that separations do produce reflections large compared to those from ply layers at the same depth.

To go beyond the mapping of separations, one must think in terms of gating out a portion of the reflection signal corresponding to the reflection at a particular interface, or from a particular laminar component. A C-scan image could then map the condition of the component or interface of interest over the surface of the tire.

Since the resolution of the laminar structure of the tire in the thickness direction is marginal at best, gate widths and time-positioning would be critical. Special timing and TVG circuits involving scan-programming and perhaps range-tracking would be required to accommodate variations in shape and thickness as the tire is scanned.

A further difficulty is that a single C-scan recording can present only a single scalar variable as a function of the two

scan coordinates. If several interfaces or laminar components are to be monitored, separate C-scan images must be produced, either by repetitive scanning or by employing a multichannel system in which several facsimile recorders make C-scan recordings corresponding to different depth intervals in the tire.

The simplest way to produce a B-scan display is to disconnect the reflection amplitude signal from the vertical deflection input of the oscilloscope and use it to modulate the intensity of the trace, which is then displaced upwards or downwards in synchronism with the one-dimensional mechanical scan. (Figure 31, to be discussed later, shows such an intensity-modulated B-scan.) To make the reflection amplitude more directly readable, however, we employ an isometric deflection-modulated B-scan technique. The display consists simply of a composite of many simple A-scan traces displaced diagonally upwards in accordance with the one-dimensional mechanical scan motion. As may be seen in figure 18, and those to follow, the effect produced is similar to that of an isometric topographic representation of a range of hills and valleys portrayed by successive profile sections.

To produce such a display, a d-c voltage analog of the scan motion is derived from a potentiometer geared to the single-axis lead screw. This voltage is added to the vertical deflection using the "A + B" display mode of a dual input unit of a Tektronix Type 556 oscilloscope. The horizontal component of the diagonal trace displacement is produced by modulating the sweep delay with the same scan voltage. This delay modulation is accomplished by adding the scan voltage to a saw-tooth pulse having fixed delay, and then triggering the delayed sweep at a fixed dc level for the sum. The technique is readily implemented using the triggering and timing circuits incorporated in the Type 556 oscilloscope. The "B-trigger" output is used to trigger the sweep of a second oscilloscope, the sweep output of which is added to the scan voltage with an operational amplifier circuit, and used to trigger the delayed sweep adjusted for a dc triggering mode.

For longer B-scans, the equivalent result can be obtained by recording the repetitive A-scan sweeps on a strip film camera. This method is described by Krautkramer[9] and attributed to Martin

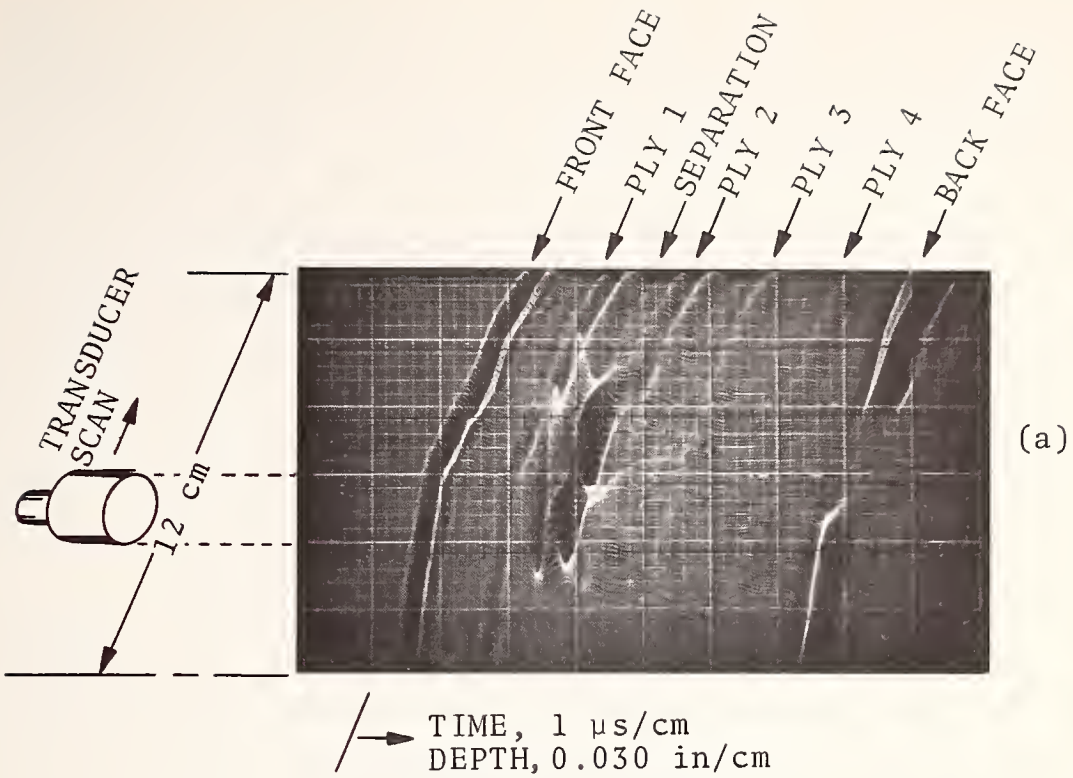

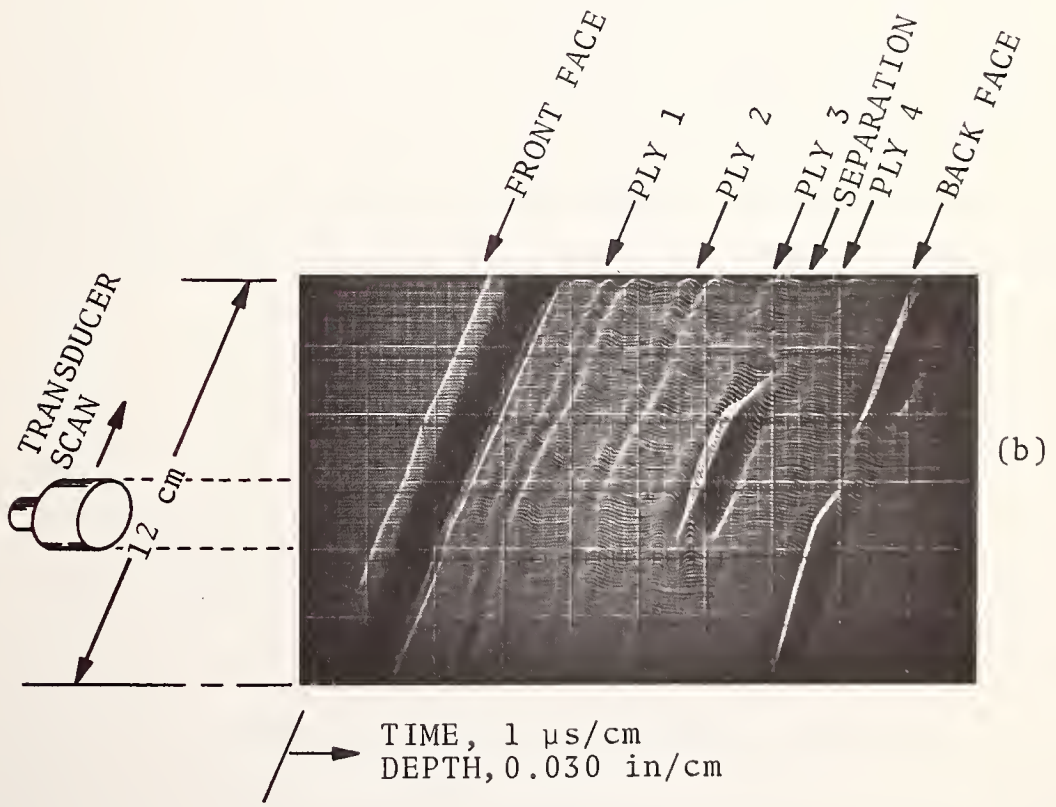

Figure 18. Separation in a Four-Ply Slab Sample (5-MHz Transducer, Step Excitation)

and Werner.[14] Such recordings can now be made by "fiber-optics coupled" recording oscilloscopes using a dry developing process. An intensity modulated B-scan recording can be printed on a conventional facsimile recorder, but such instruments are not fast enough to record the data directly. Either the scanning process would have to be slowed down to permit use of sampling techniques, or the data would have to be buffered by some device such as a television scan converter. As discussed in Reference 2, recording oscilloscopes are available which have sufficient speed and information handling capacity to serve a multi-transducer scanning system which would make this recording technique reasonably economical.

In the paragraphs to follow, isometric deflection-modulated B-scan displays produced as described above are presented which illustrate the nature of the display for various defects and structural features built into slab specimens. Thereafter, similar displays will be presented showing a naturally occurring separation in a worn tire. C-scan recordings are not presented because a two-dimensional scanning system was not available. As discussed above,[2] it is considered that C-scan recordings can be made in a practical way for tires, but the B-scan display is preferred, at least in the initial phase of application in tires, because its richer information content makes it possible to interpret results without ambiguities.

5.2 SEPARATION IN A FOUR-PLY SLAB

Figure 18 shows amplitude-modulated isometric B-scans of an artificially introduced separation in a four-ply slab sample. Clearly resolved reflections from the four cord layers are obtained.

The upper photograph shows the separation between plies 1 and 2, as seen when the sample was inspected from the side nearest the separation. The lower photograph shows the separation between plies 3 and 4, as seen with the sample turned over. It is submitted that both the lateral location and the depth of the separation would be tolerably apparent, even to an untrained observer. The acoustic shadowing of the region beyond the separation is also quite apparent.

Advantage has been taken here of the fact that the polarity of the dominant reflection from the separation is opposite to that from the water/rubber interface. The air film at the separation represents a marked decrease in acoustic impedance while the water-to-rubber interface represents a transition from a lower to a higher acoustic impedance. Thus, the reflection coefficients given by Equation 3-5 have opposite sign, and the polarity switch on the oscilloscope vertical axis can be positioned to make the reflection from the separation rise up from the ground level of the display rather than disappear down into it as does the front face reflection. Up-going reflections have been enhanced somewhat by applying the reflection signal simultaneously as an intensity modulation of the trace.

The apparent warping of the reflecting surfaces in figure 18 represents a real buckling of the slab sample in the test fixture. The departure from flatness corresponds to approximately 0.5 microseconds in round-trip time, indicating that the surface buckle is approximately 0.015" across the 4 3/4-inch scan. Thus, this display technique is very sensitive for indicating non-uniformities of thickness or departures from smooth contours.

5.3 PLACEMENT OF REINFORCING MATERIALS

Figure 19 illustrates the capability of the B-scan technique for providing information as to the placement of reinforcing materials in the tire. As illustrated in the construction sketch, the test piece simulates a belted tire in which the outer ply of the two-ply belt is misplaced, to give a variable degree of underlap for the lower ply. Using a 5-MHz 3/4"-diameter transducer, the displays clearly show the location of the belt edge itself. Furthermore, the edge of the belt appears sharper where the underlap is smaller. Obviously, discrimination of such features could be greatly improved by use of a focused transducer; however, it is satisfying to find that some useful information could be obtained even with a non-focused transducer.

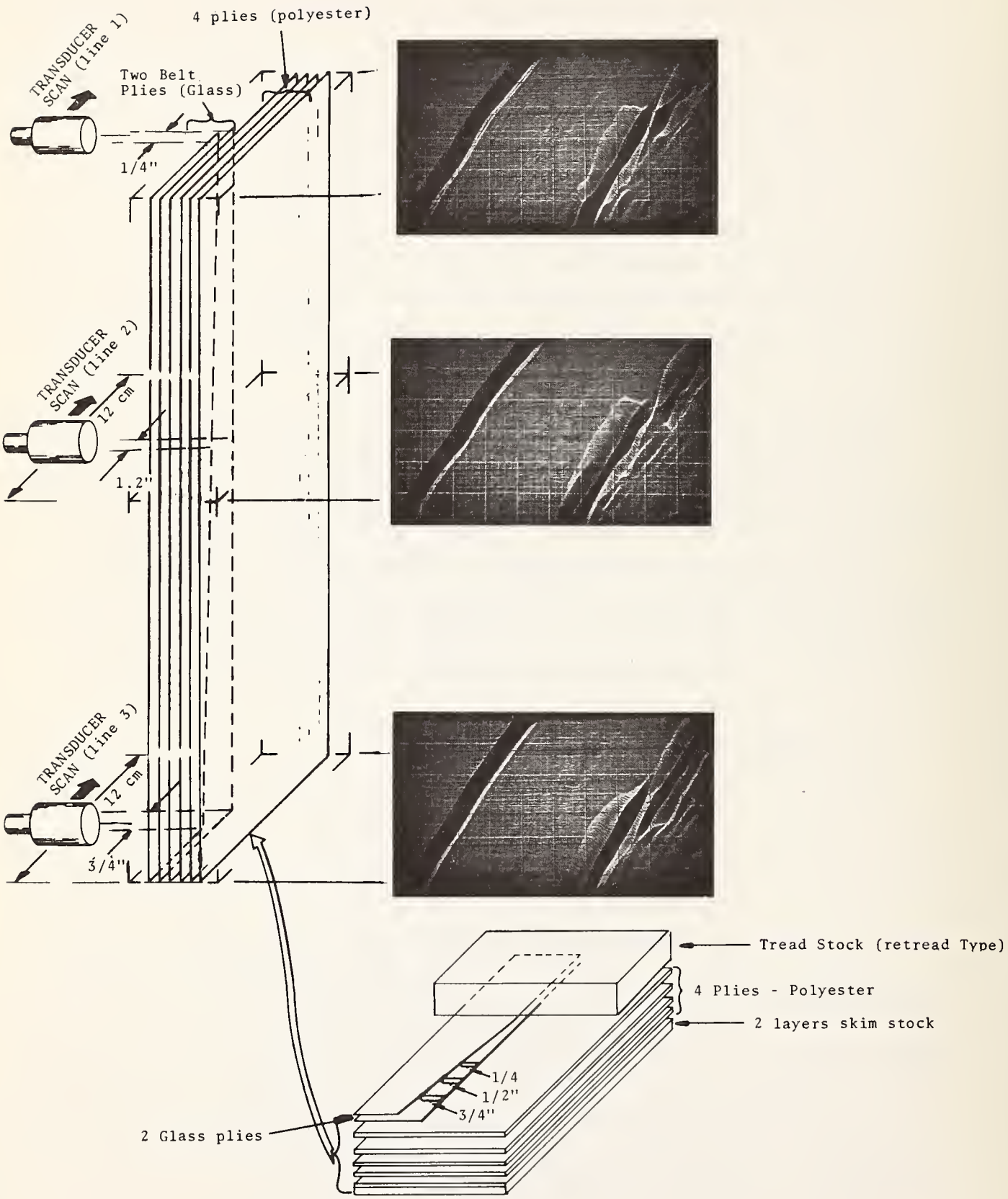

Figure 19. Underlap Variations on Belt Edge (5-MHz Transducer)

Figure 20 shows another illustration of an anomaly in placement of reinforcing materials. In the central region of the scan, the upper ply is doubled in a 1" region of overlap. (This is not a simulated tire splice, since in the overlap regions the ply cords cross rather than lie parallel.) The presence of the anomaly is readily apparent.

5.4 GAUGING OF INTERNAL GEOMETRY

Figure 21 illustrates the power of the B-scan display to reveal even minor variations in internal geometry. A scan is shown of the tread-rubber/carcass-rubber interface, taken from the carcass rubber side for convenience. With the expanded time scale employed, (0.5 μs/cm or (0.15 in/cm)) it is clear that the otherwise smooth plane of the interface is displaced by a depth variation of about 0.007". At one point, the interface is displaced in depth by roughly one quarter of the ultrasonic wavelength, within a distance comparable to the beam cross section, and as the beam straddles the depth displacement, the return signals from the higher and lower regions of the fault are one half wavelength out of phase and cancel each other. In this case there is no confusion with a change in reflection, because the depth-offset nature of the fault is readily apparent from the B-scan display. Figure 22 shows additional B-scans taken along two lines 1" apart crosswise to the extrusion direction of the tread stock. The data were taken to determine whether rubber flow during curing might have caused the interface to follow the shape of the extrusion, and the displays confirmed that it had not done so to any significant extent. However, these displays illustrate the sensitivity of the technique for revealing minor variations in the amplitude of a reflection from an interface.

5.5 THICKNESS GAUGING

The power of reflection techniques for thickness gauging is demonstrated in readily appreciated terms in figure 23, which shows B-scans passing over single and double thicknesses of familiar

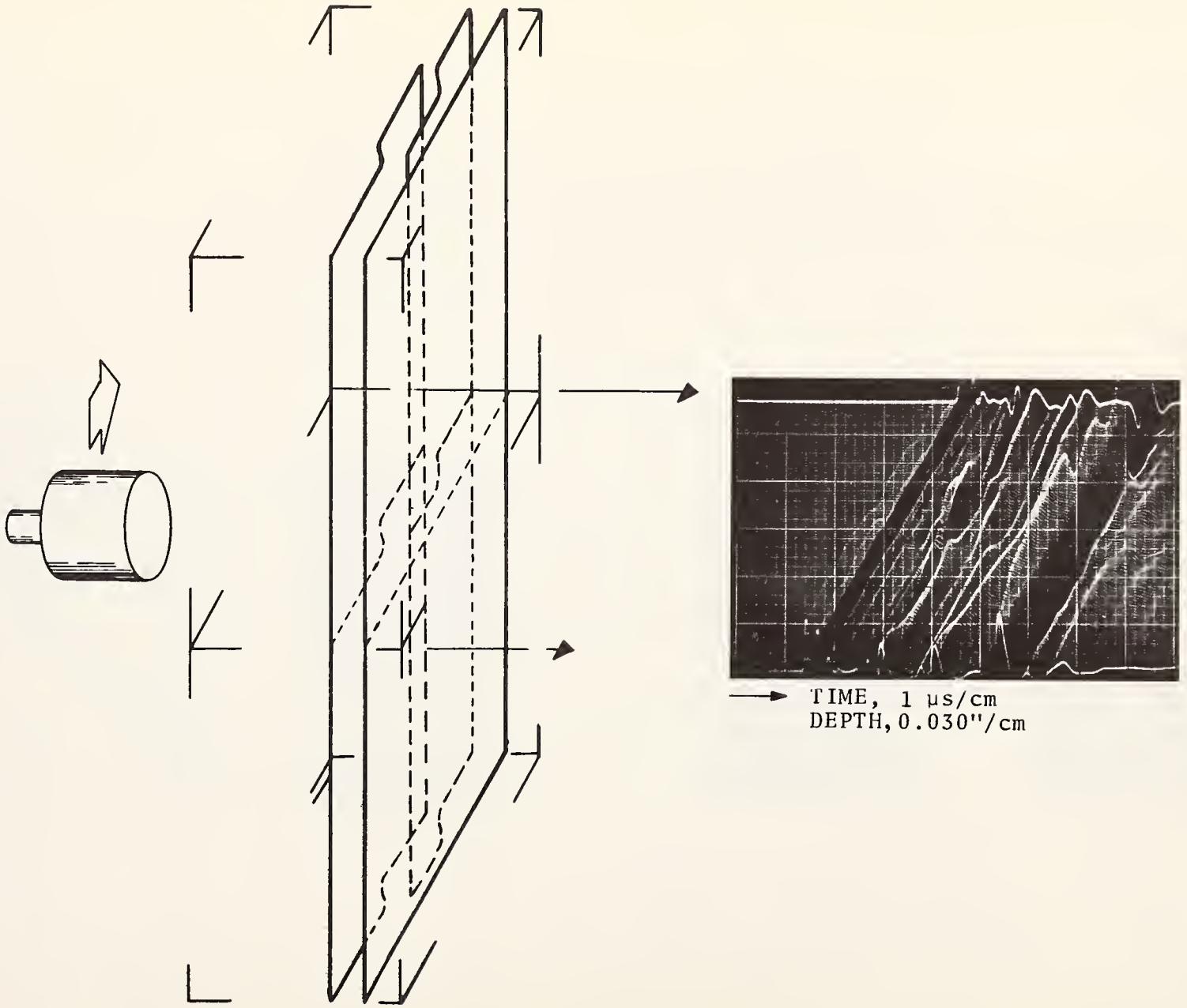

Figure 20. Ply Overlap
(5-MHz Transducer)

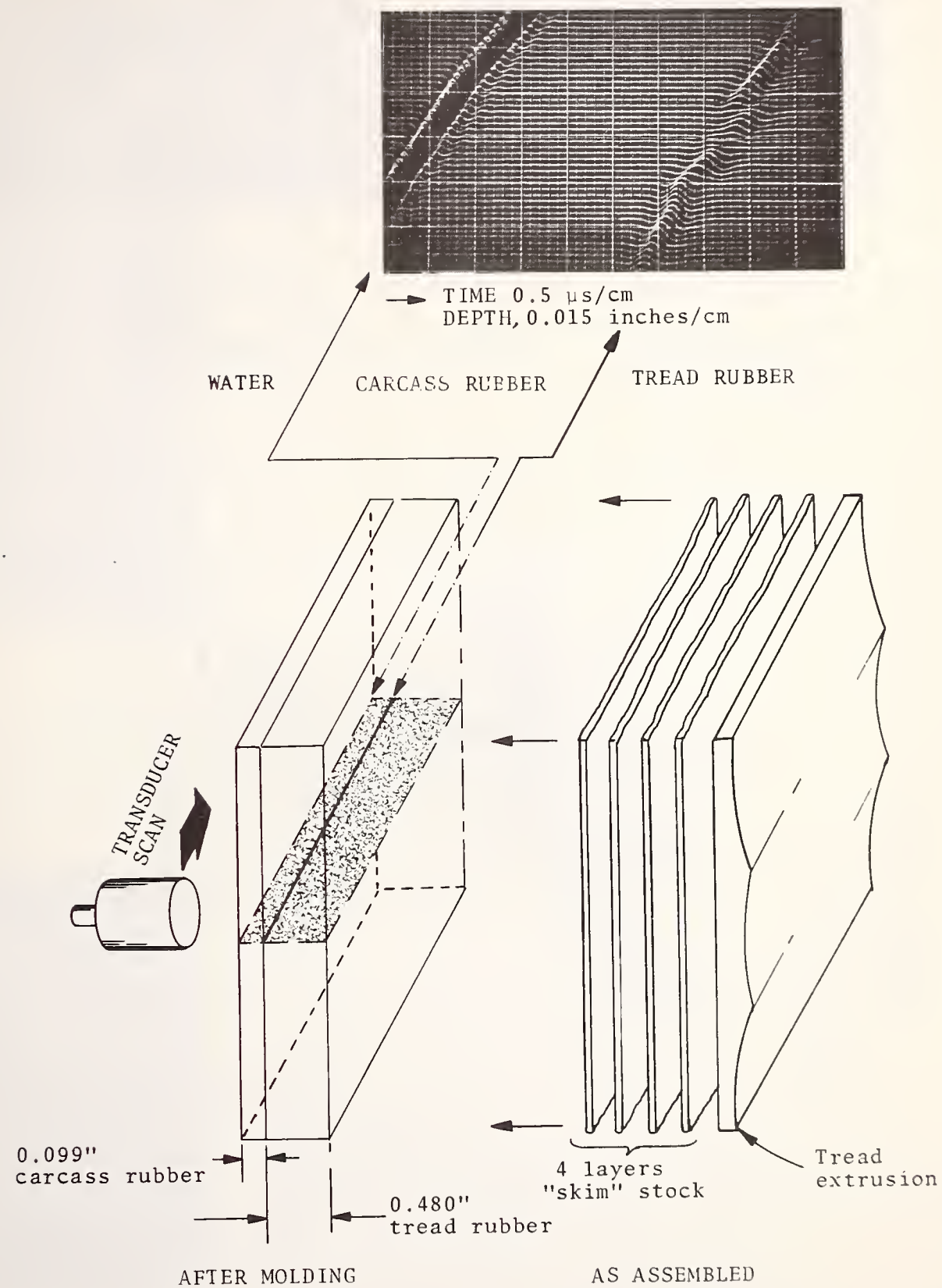

Figure 21. Carcass Rubber to Tread Rubber Interface---B-scan Parallel to Extrusion Direction (5-MHz Transducer)

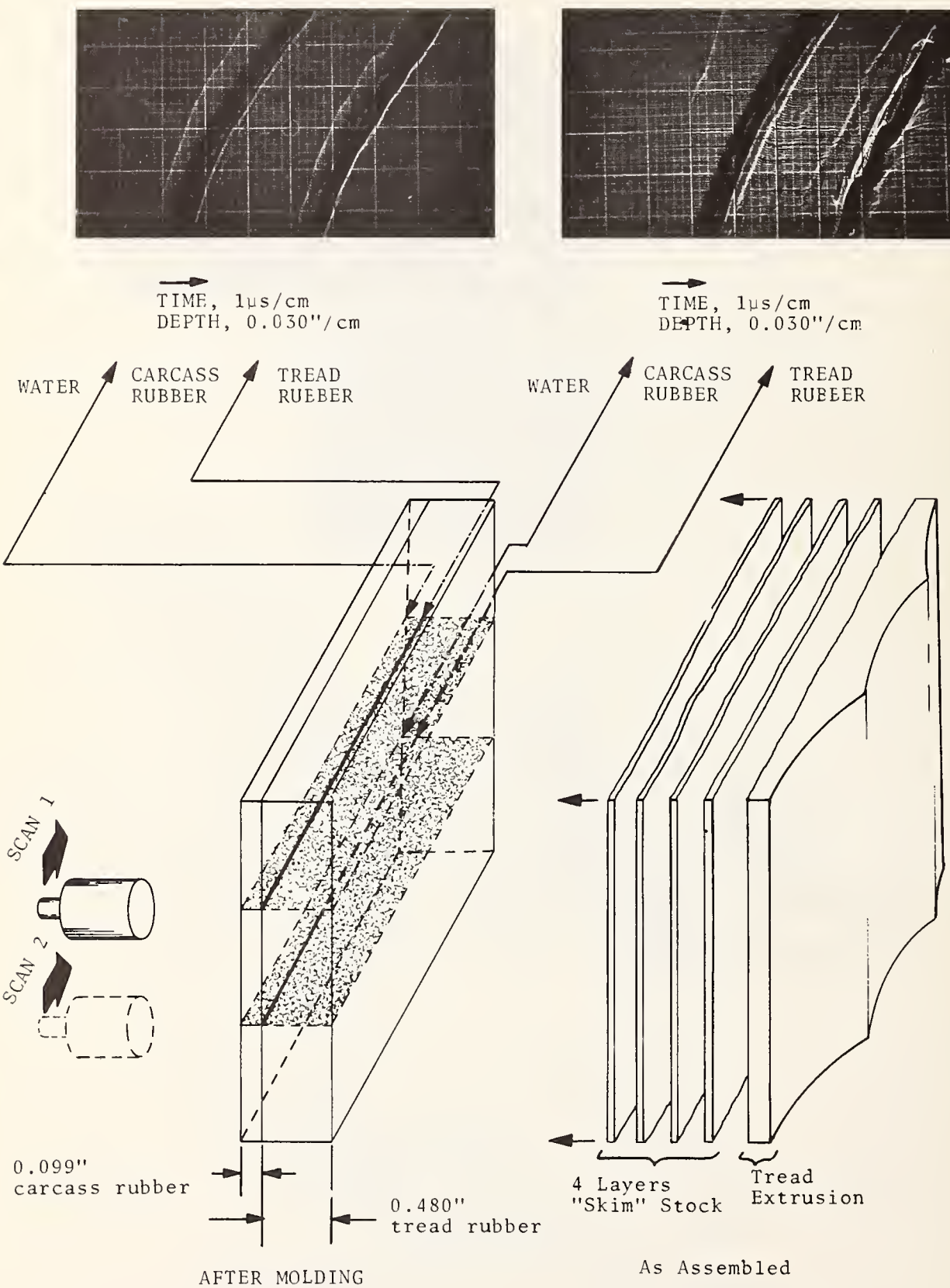

Figure 22. Carcass Rubber to Tread Interface---B-scan Transverse to Extrusion Direction (5-MHz Transducer)

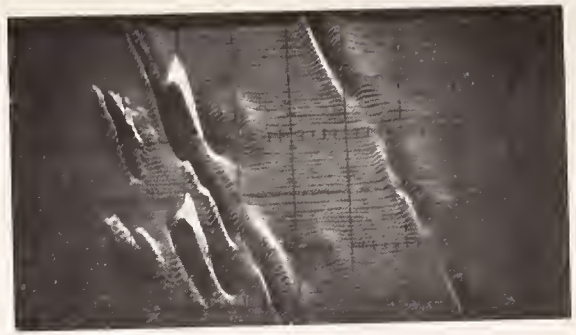

TIME, 1 μs/cm
DEPTH, 0.030"/cm

TIME, 1 μs/cm
DEPTH, 0.030"/cm

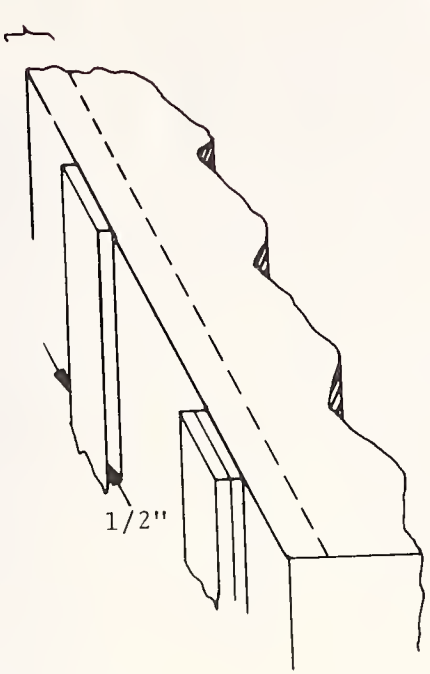

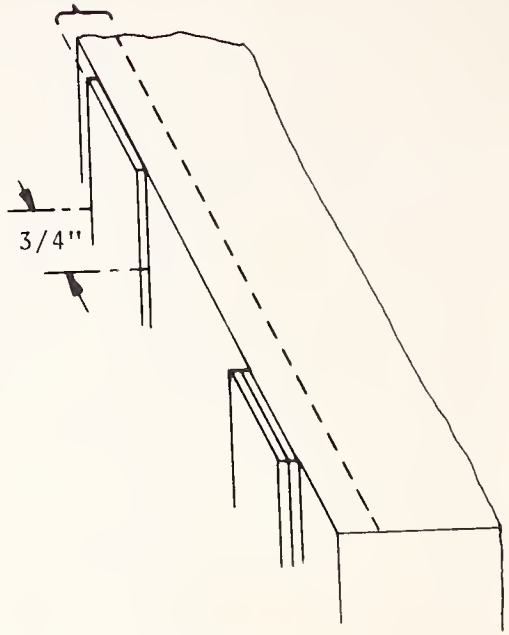

Plastic Tape
Single & Double Layers
0.008" thick x 1/2" wide

Rubber Tape
Single & Double Layers
0.032" thick x 3/4" wide

Figure 23. Thickness Resolution
(5-MHz Transducer)

varieties of electrical insulating tape applied to the surface of a slab sample. The thickness step of a single layer of 0.008" plastic tape is quite apparent, as is the distinction between single and double layers. As compared to the plastic tape, the rubber tape shows only a small reflection at the tape/slab interface, consistent with the better impedance match of more similar materials.

5.6 DETECTION OF ANOMALOUS BONDING

The central display in figure 22 reveals a subtle reflection from an interface which is not supposed to exist, namely one between two of the four layers of skim stock from which the carcass rubber layer was assembled. Note that the anomaly is localized. It does not appear on either of the other scan lines.

In figure 24 we see that all of the joining interfaces in a thick piece of carcass rubber assembled from 12 layers of skim stock are detectable using the 5-MHz transducer. These reflections

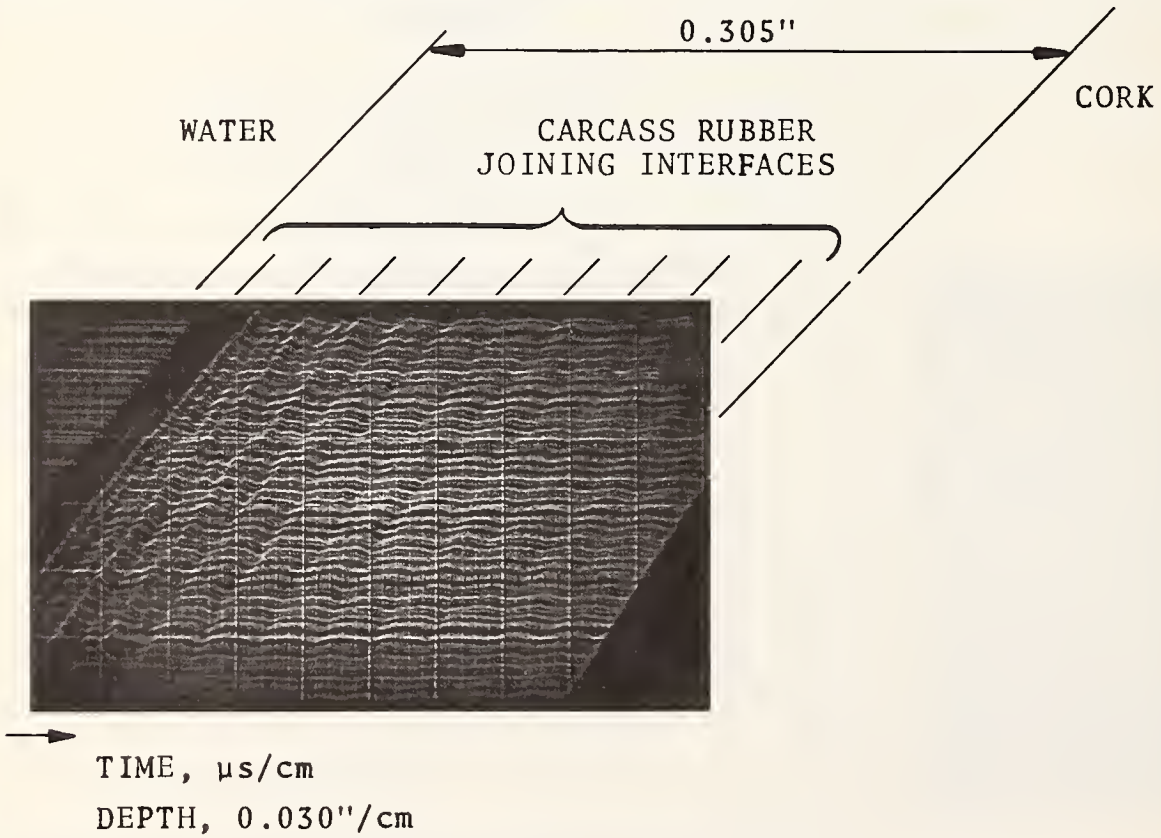

Figure 24. Joining Interfaces in Carcass Rubber Molded from 12 Layers of Skim Stock (5-MHz Transducer - Step Excitation)

occur at "interfaces" between supposedly identical materials, and the reflections must be attributed to thin intermediate layers at the interfaces, having slightly different properties, presumably because of diffusion of constituents to the surface, surface oxidation, or slight surface contamination.

To further check the capabilities of the technique for detecting subtle interfaces and weak bonds, a slab sample was made up of six layers of skim stock with two 1"-wide strips of precured material substituted for the green (uncured) material in the central portion of the two inner layers. Figure 25 presents three B-scan displays together with a sketch showing the construction of this sample. The lower display shows the result in the normal part of the slab, where six layers of previously green rubber have bonded together in the curing process. The center display shows the result of a scan down the center where the strips of pre-cured rubber are embedded. The reflection at the boundary between the green rubber and the pre-cured rubber is uniform, indicating that uniform bonding has occurred, but showing a difference in acoustic impedance for the double-cured stock, as compared to that subjected to only one curing process. The junction between the pre-cured strips appears to be separated except at the lower end of the scan, where a much smaller but clearly observable reflection occurs, even though the junction is between identical materials. At the gain setting employed in the lower two displays, green rubber-to-green rubber interfaces do not show. The upper display shows, however, that with sufficient gain (32 dB more), even such interfaces give obvious reflections.

5.7 SEPARATION IN A TIRE TREAD SECTION

But one may well ask whether these scanning and display techniques are practical in the face of the complex surface relief and internal structure of tires. Proof that these factors do not preclude use of such techniques is provided by figure 26, which shows B-scans taken in the rotation direction in the tread region of a tire. The upper display shows results of a scan over a sound region of the tire, while in the lower display, evidence

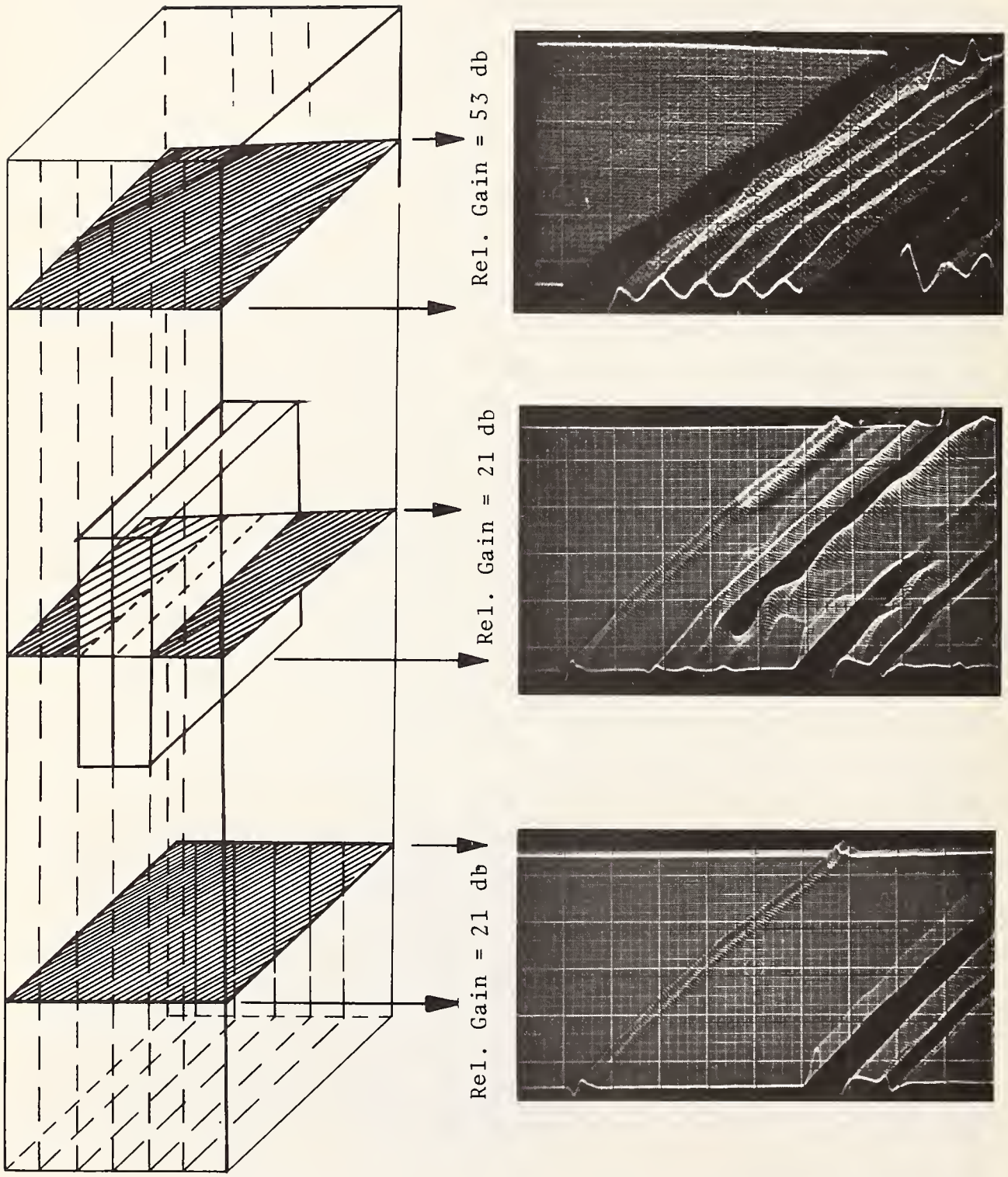

Figure 25. Six-Layer Slab Sample with Two Layers of Pre-Cured Material in an Embedded Strip (5-MHz Transducer-Step Excitation)

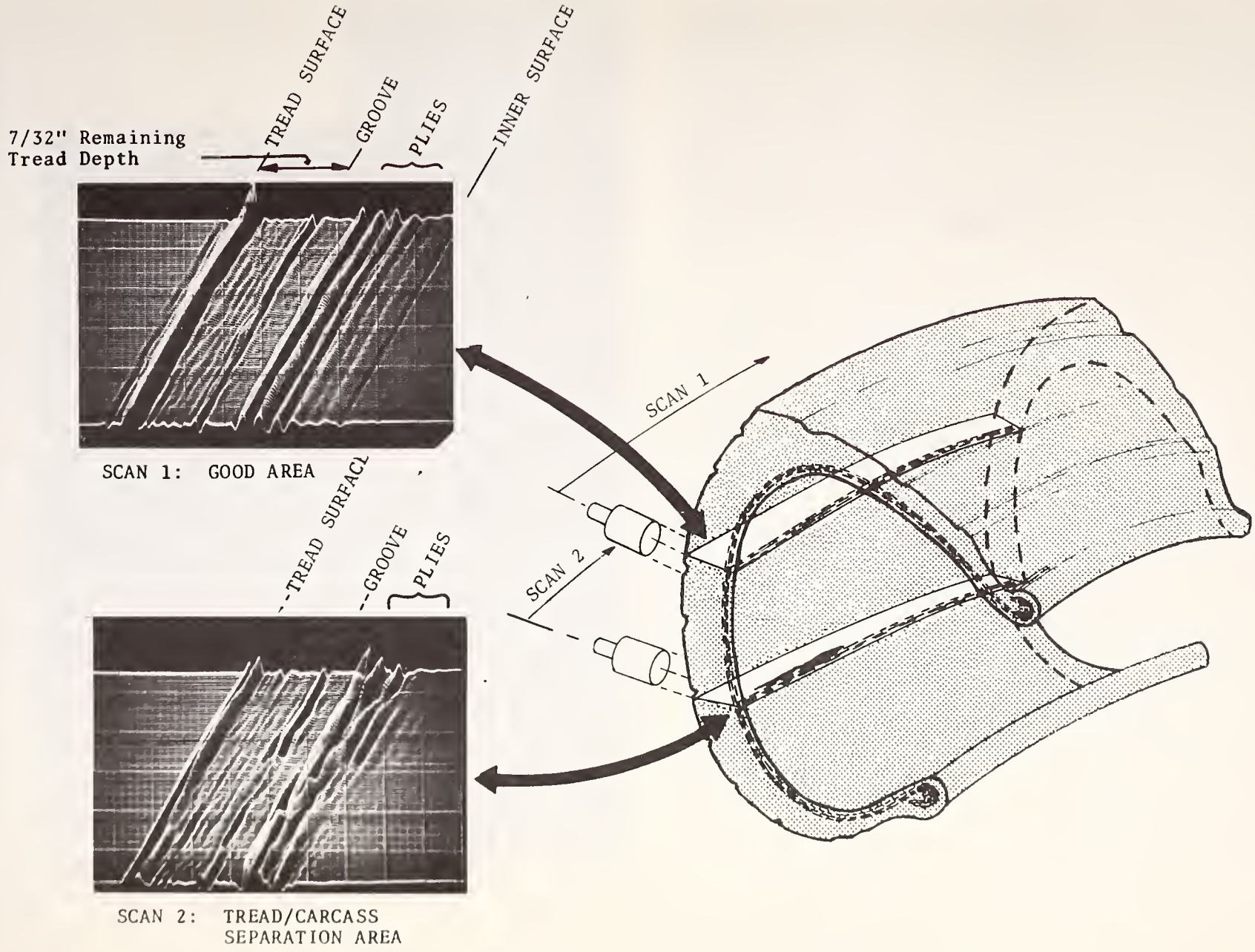

Figure 26. B-Scans of Tire Section Showing Tread/Carcass Separation

of a tread/carcass separation is visible just below center of the scan. To make the test, a portion cut from the tread was flattened by bonding it to an aluminum plate using contact cement, as shown in figure 27. The sample was cut from a used glass-belted tire which had failed in service, and other tests on portions from this tire showed a high incidence of separations. The remaining tread depth is readily gauged from the ultrasonic display by measuring the time from the principal reflection at the water/tread interface to the tread groove bottom. The time delay of 7.2 microseconds indicates a remaining usable tread depth of about 7/32". As may be seen in the photograph (figure 27), the tread surface was very irregularly worn, contained embedded pebbles, etc. As might be expected, this worn tread surface generates a very rough and irregular pattern at the initial water/tread interface. From this point down to the bottom of the tread groove, the upper display shows minor undulations corresponding to scattering from surface relief features at corresponding depths in the tread pattern. Despite the surface roughness, the belt and body ply reflections in the upper

Figure 27. Worn Tread Section Scanned in Figs. 26, 29, 30, and 31.

display are quite uniform along the direction of scan, whereas in the lower display, these reflections are strongly disturbed. A detailed analysis accounting for all the disturbance in terms of structural anomalies in the tire would be a formidable task, but such analysis is completely unnecessary to appreciate the contrast between the normal pattern above and the abnormal pattern below. One aspect of the disturbance, however, proves very simple to interpret. Note that in the upper display, the region between the tread groove bottom and the first belt ply reflection is relatively smooth and uncluttered, whereas the lower display shows a strong reflection in this region just ahead of the belt ply, just below the center of the scan. The fact that the pulse polarity is opposite to that of the water/tread reflection tells us that this reflection is from a low impedance anomaly and is in all probability a tread/carcass separation. The interpretation of the anomaly as a separation is supported by the interferometric hologram reconstruction shown in figure 28.

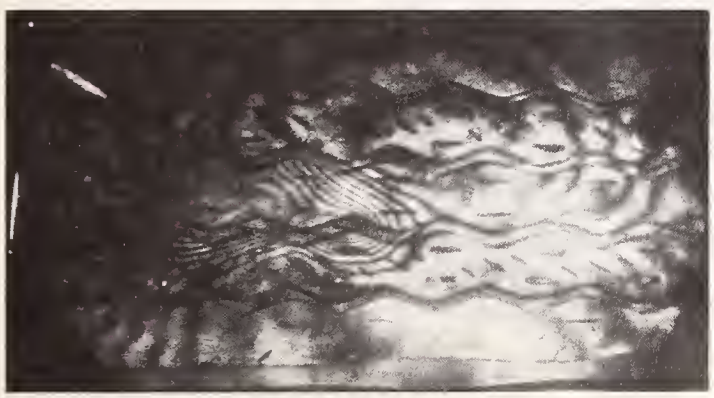

Figure 28. Holograph Confirmation of Tread/Carcass Separation Indicated by Reflection Ultrasonics

5.8 FOCUSED TRANSDUCER FOR IMPROVED LATERAL RESOLUTION

The preceding displays have been obtained with a 1" diameter 1-MHz plane-wave transducer, and the apparent extent of the separation in the rotational scan direction is close to the size of the acoustic beam which defines the spot-size. Figure 29 shows detailed displays of this separation, the upper display being obtained with a focused transducer, having a 3" focal length in water. The 1" diameter of this transducer is a bit small for its operating frequency (0.4 MHz), being only about 6.7 wavelengths. Nevertheless, it has a smaller beam diameter in the focal zone than

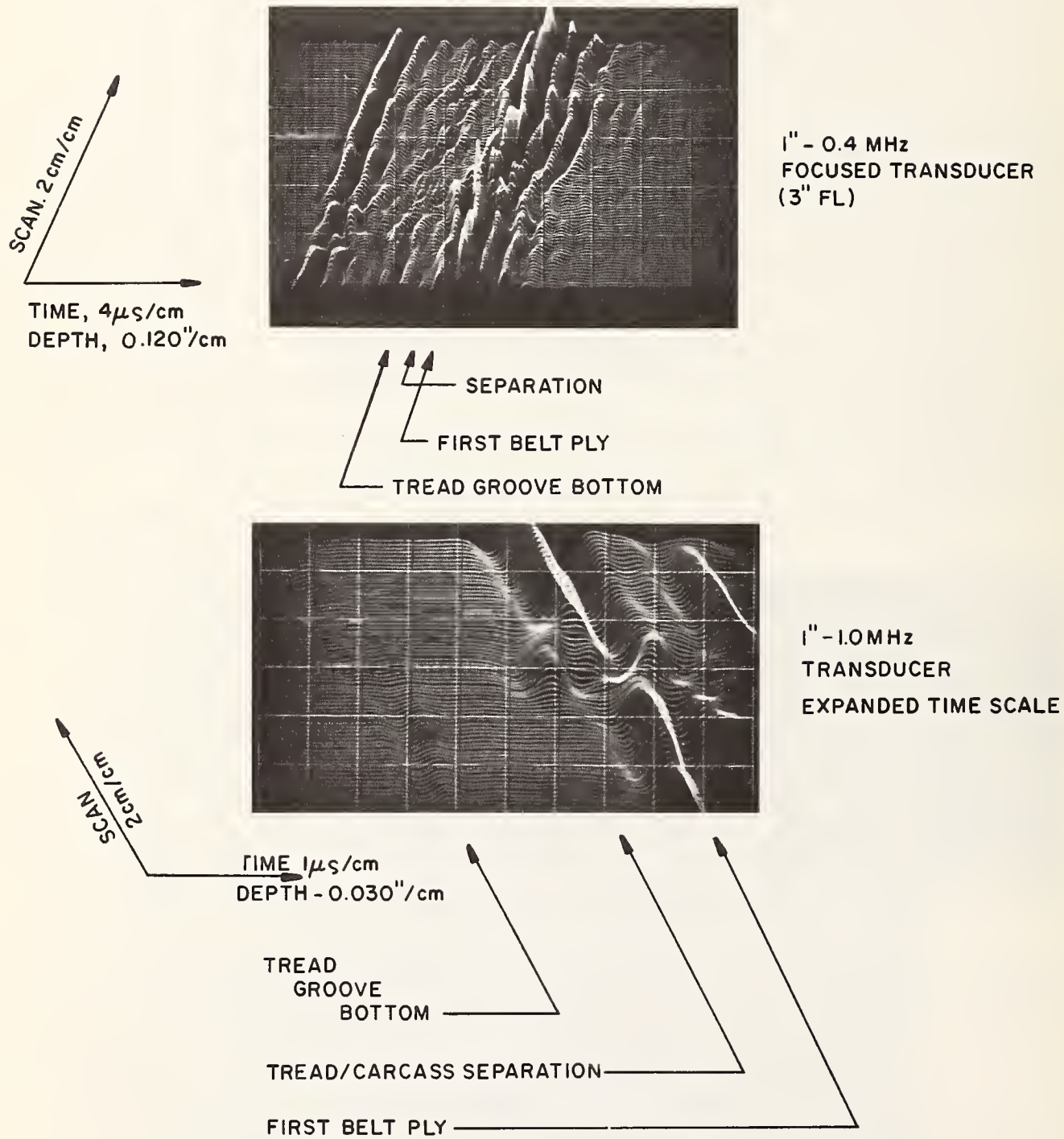

Figure 29. Tread/Carcass Separation Seen with Higher Resolution

the 1", 1-MHz transducer, and hence offers improved lateral resolution. It is interesting to note that the belt ply reflections appear about the same, indicating that the reflection pattern is characteristic of the ply structure itself. The lower display shows a more detailed view of this region, again with the plane-wave 1-MHz transducer, but at an expanded time scale and with lower deflection amplitude. Here the isometric slope is taken to the left, so that the reflection from the separation will not be obscured behind the ridge produced by the belt ply reflection. Here it is quite clear that this reflection occurs in the otherwise reflection-free region of clear rubber between the tread groove bottom and the outer belt.

Figures 30 and 31 show complete sets of scans taken on the tread section discussed above. Successive scan lines are spaced 0.350" apart, being approximately centered over successive grooves and ribs in the tread pattern. As in the lower display of figure 29, the isometric slope in figure 30 has been taken to the left, so that the separation of interest will appear in front of the ply reflections rather than behind them. The displays in figure 31 are of the ordinary intensity modulated form. Their rectilinear format makes it easier to read the depth of an anomaly, but the deflection-modulated isometrics provide a powerful technique for revealing minor amplitude and phase variations in the complicated reflection signal.

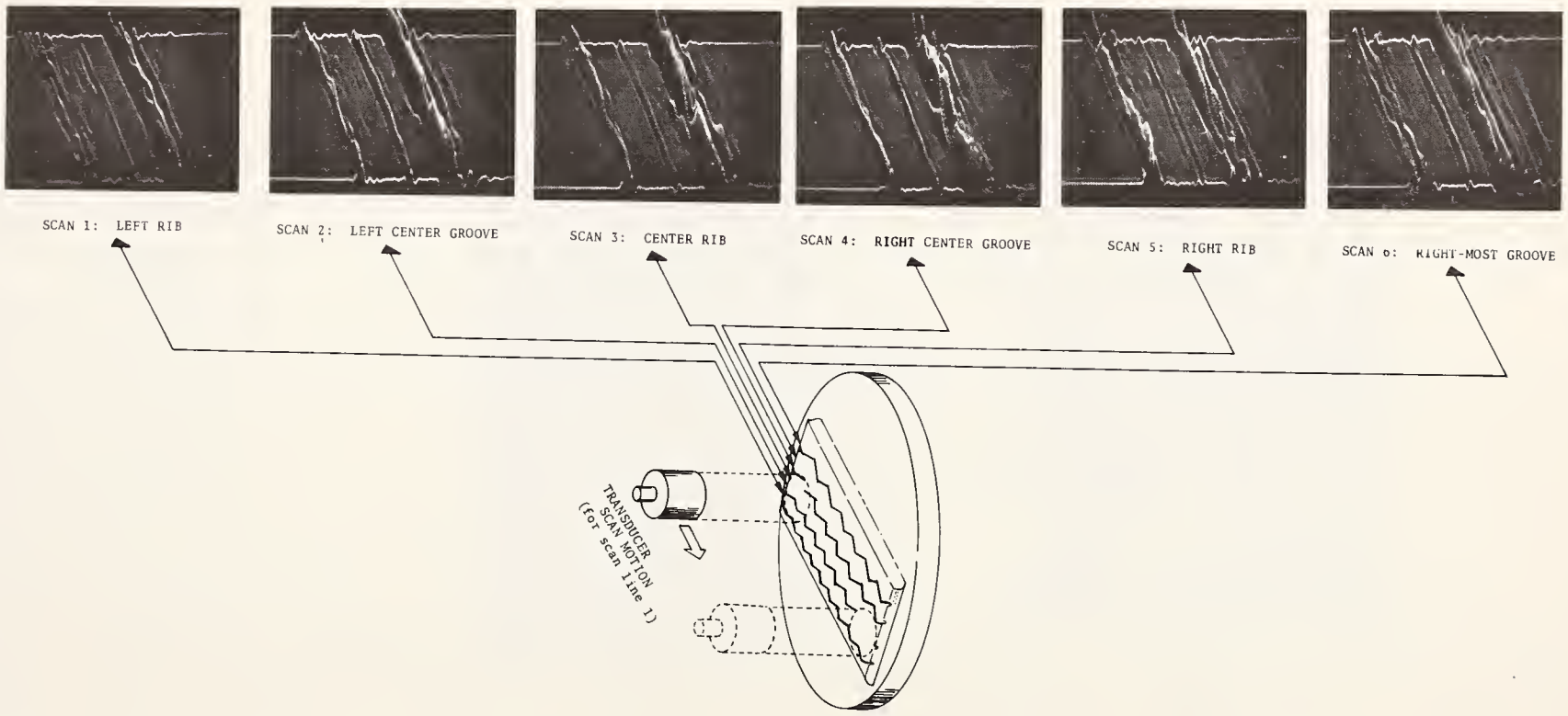

Figure 30. B-Scans of Tire Tread Section--Complete Set, Isometric Displays (1-MHz Transducer)

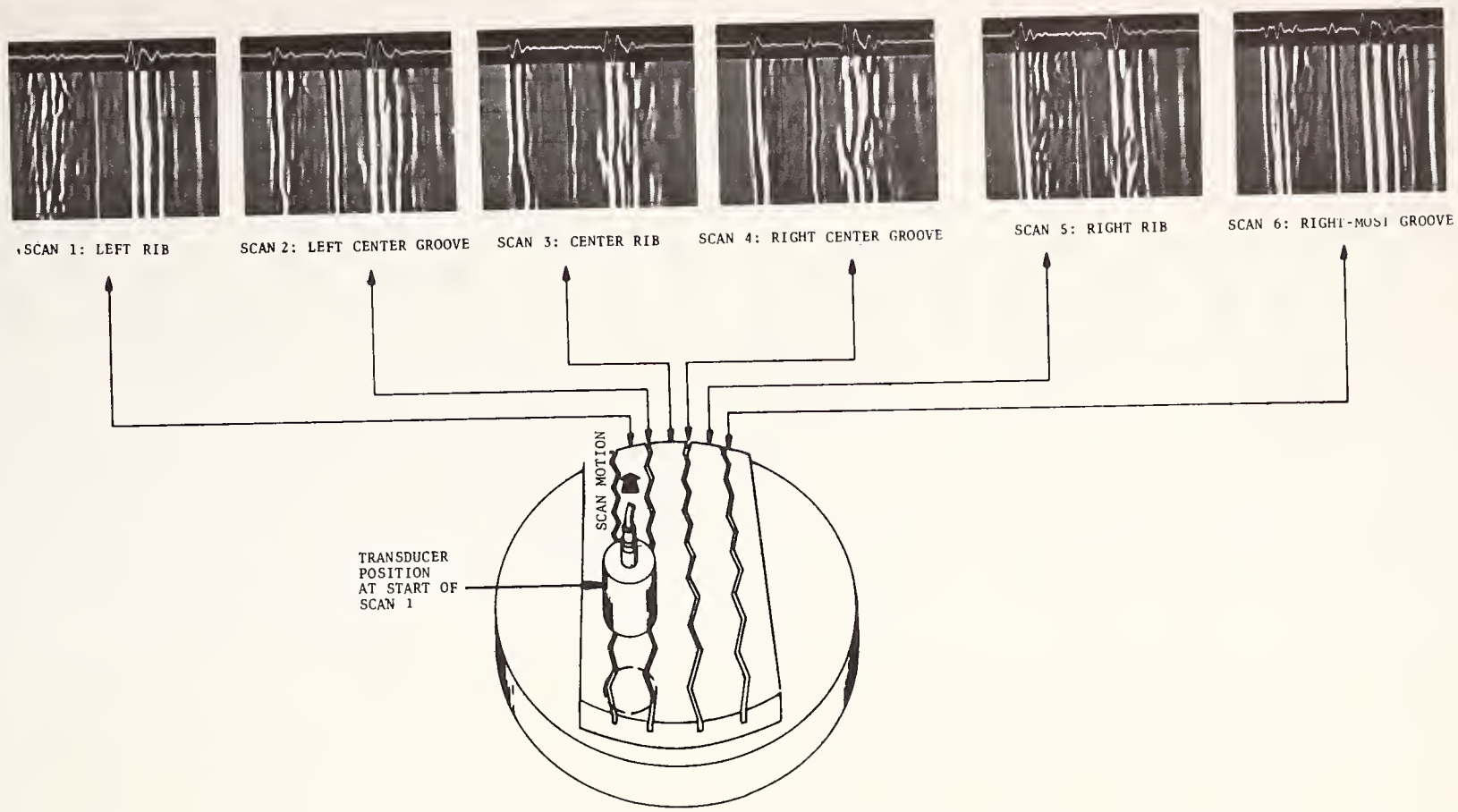

Figure 31. B-Scans of Tire Tread Section--Complete Set, Intensity Modulated Displays (1-MHz Transducer)

6. CONCLUSIONS AND RECOMMENDATIONS

A-scan reflection signals and B-scan displays have been presented for a number of slab specimens made from tire component materials and exhibiting various defects and anomalies of structure. These data clearly show that modern pulse echo ultrasonic techniques employing short pulses from highly damped transducers, with fundamental frequencies in the range 1- to 5-MHz, are capable of definitively characterizing the laminar structure of such samples, and will reveal the presence and nature of defects ranging from gross separations to subtle variations in interface bonding. Various defects and structural anomalies generate characteristic patterns on image-type displays, which are readily interpretable with a minimum of explanation.

If we were concerned exclusively with similar laboratory specimens, there is no question but that a strong capability both for detecting and characterizing defects and structural anomalies has been conclusively demonstrated. However, in many ways the capabilities demonstrated for laboratory samples apply to idealized cases seen under ideal or simplified conditions, and we are interested really in estimating the capabilities of the technique for detecting similar anomalies in actual tires. At present, no data is available demonstrating the detection of real defects in whole tires, but rather we have available limited data on small sections cut from actual tires. These data do, however, provide a realistic indication of the loss of signal strength and time resolution resulting from the propagation of short pulse ultrasound through tire materials, and give some idea of the magnitude and variability of the background reflections caused by normally present structural components. In the paragraphs to follow we will attempt to integrate the information available from the slab specimen data and that available from the tire section measurements to indicate the level of capability to be expected in tires.

In a general way, time resolution and signal strength are progressively decreased for greater depths of penetration into the tire. In the outermost regions of the tire, down roughly to the

outermost ply layers, the level of capability may be expected to approach that demonstrated for slab specimens, and capabilities will be progressively degraded for greater depths of penetration. However, it is to be noted (figure 13) that returns some 50 dB above noise have been observed from the inner surface in the six-ply tread region of a double-belted tire. Thus, at the maximum depths of penetration involved in passenger tires, some level of capability will be available. The paragraphs to follow discuss these factors more specifically with respect to various kinds of capability.

For heavier tires, as used on trucks, buses, aircraft, or construction equipment, transducers of somewhat lower natural frequency can be used as necessary to obtain adequate penetration. Presumably, it would be sufficient to obtain depth resolution bearing the same proportion to tire thickness as for passenger vehicle tires. This criterion would permit the transducer frequency to be lowered in inverse proportion to the tire thickness. Since attenuation varies generally as the square of the frequency, penetration would then be improved in even greater proportion than necessary.

6.1 SEPARATIONS

Outright separations of size comparable to the acoustic beam cross section (say 1/2" or larger) should be readily detectable at any depth within the structure. The reflection will be essentially total if the separation contains a layer of gas a few microinches in thickness, which will certainly be the case for any separation which would give a definite fringe pattern by holographic interferometry. Since such separations will give large signals compared to the background reflection from the ply structure, they can be detected by simple amplitude discrimination, a process which could be easily automated. The depth of such a separation should be measurable to about .020" in the deepest regions of a tire or to within 0.001" at the outermost cord layer. Thus, a very good estimate should be available as to which interface has separated, even if individual cord layers are not completely resolved.

6.2 POROSITY

Porosity should be readily detectable at any depth in the tire. Porosity causes heavy attenuation of the signal resulting in the disappearance of the back face echo, the amplitude of which can easily be monitored in the thickest regions. Since a porous region will essentially eliminate the normally present returns from any structural element lying below it, some estimate of the minimum depth of a porous region should be available.

6.3 THICKNESS MEASUREMENTS

Thickness and depth measurements can be made with precision ranging from about .001" at the shallowest depth to about .020" at the greatest depth of penetration, provided that a clean return is available from a well-defined interface. (These figures assume that a time measurement can be made to 1/5 of the fundamental pulse period which can readily be as short as 0.2 microseconds in the outermost region but is degraded to as much as 3.5 microseccnds at the deepest penetration.) The total thickness of tread and/or carcass rubber outside the outermost ply or belt should be measurable to a few thousandths of an inch, and similar precision should be attainable for measurement of tread pattern depth. A very sensitive monitor of the thickness uniformity of all elements in the laminar structure can be provided by the B-scan techniques described here. A B-scan taken in the direction of rotation of the tire should generate a display consisting of a uniform set of parallel lines, and departures from this pattern should provide a very sensitive indication of splice quality.

6.4 PLACEMENT OF CORD MATERIALS

Cord materials give observable contributions to the reflection signals at all depths. Therefore, a full capability for detection of errors in placement of reinforcing materials (figures 19 and 20) will be realizable throughout the tire.

6.5 INTERFACES BETWEEN DIFFERENT RUBBER COMPOSITIONS

Slab measurements (figure 13) show that the interface between tread and carcass rubber is readily detectable through a reasonable thickness of tread rubber, so far as signal-to-noise ratio is concerned; however, the reflection from a well-bonded interface is small in amplitude compared to the normally present ply reflections or the water-to-rubber interface at the bottom of the tread pattern. At a sufficiently high gain setting, the position of this echo should be readily evident on a B-scan recording. Based on admittedly limited observations, it appears that selection of this echo as a reference point for thickness measurements or for monitoring of its amplitude would pose rather severe problems in control of gate timing. With the B-scan technique, however, one does not need to know in advance where to look, and with a sufficient gain setting, it should be possible to monitor both the depth and amplitude of the reflection from this interface.

6.6 CURE STATE

Slab sample measurements (figure 25) verified that variations in cure state alter the acoustic impedance of tire rubbers, as would be expected. Where rubber stocks of the same composition having differences in their state of cure are bonded together, a reflection occurs at the resulting impedance discontinuity. Perhaps an analogous situation could occur in a tire if some of the component materials were scorched in the calendering operation or if some composition were in error so that one component of the tire was overcured by a cure cycle which was proper for other parts. On the other hand, an overall error in curing treatment would affect either the whole tire or a large region thereof, thereby altering the cure state of more than one laminar component. One would still expect variations in the reflection coefficient at the interface between different rubber compositions, since it would be very fortuitous if two different kinds of rubber changed acoustic impedance with cure state in exactly the same way. In the case of gross overcure or undercure of an entire tire, it is just possible that overall changes in the acoustic properties of the rubber,

particularly the attenuation, might be evidenced by changes in the amplitude of the back face reflection. The magnitude and probability of occurrence of effects such as these are admittedly matters of conjecture. However, it is clear that some potential exists for detection of variations in cure state.

6.7 WEAK BONDS

In slab specimens, weak but clearly measurable reflections are obtained from normally bonded interfaces between identical rubber stocks (figure 24). On the other hand, essentially total reflections are observed for outright separations produced by various surface contaminants (figures 11 and 18). Similar total reflections are obtained for the surface of separation between layers of rubber placed in dry contact. When bonding has been deliberately weakened by pre-curing one or both of the components joined, reflections of intermediate amplitude are observed and random variations of reflection amplitude occur indicating variability of the bond quality (figure 25). Thus, bond status can be monitored quantitatively all the way from a normal bond condition to a complete separation. However, for weak bonds in which the components joined are at least in a state of wet contact, the reflection coefficient at the interface is extremely small, and the possibilities for detecting such variations in tires depend upon the region of the tire considered. Weak bonding at a rubber-to-rubber interface outside the outermost ply (such as the tread rubber/carcass rubber interface) should be almost as readily detectable in a tire as in a slab specimen. In other regions, the effectiveness of the technique will be determined by the level of interference from the clutter background of reflections from the internal structure normally present. However, it is not necessary that the defect signal be large compared to the normal background--it is only necessary that the disturbance of the background be detectable. The isometric B-scan displays presented in this report show that this display technique provides a very powerful means for detecting very small perturbations of a regular pattern of

reflections. The ultimate effectiveness of this technique for detecting the rather subtle indications of weak bonding will depend on how much the normally present reflections due to internal structure fluctuate as the tire is scanned.

To summarize, then, it is reasonably well established that high resolution reflection techniques would have a high level of capability for detection of gross structural anomalies such as outright separations, dimensional irregularities, misplacement of reinforcing materials, etc. Other techniques, including through-transmission ultrasonics, are competitive with respect to detection of some of these, but the capability for characterizing defects and laminar structures in the thickness dimension is unique. Furthermore, a unique potential has been demonstrated for reflection techniques for detecting relatively minor variations in interface conditions associated with weak bonding. The approach suggested is that of looking for abnormally large variations in the amplitude and/or phase of the observable background reflections due to the normal laminar structure of tires.

The effectiveness of the suggested approach will depend crucially on the level of natural variability of the reflections from normal internal structure. It is, therefore, recommended that an immersion scanning capability be implemented to evaluate the validity of the technique.

7. REFERENCES

1. Litant, I.,"Nondestructive Tire Inspection Studies at the Transportation Systems Center," paper presented at Akron Rubber Group Winter Symposium, January 28, 1972.

2. Ryan, R.P., Design Considerations for an Ultrasonic Pulse-Echo System for Inspection of Automobile Tires (to be published)

3. Halsey, G.H., (Scientific Testing Laboratory, Indiana, Pa.), "The Nondestructive Testing of Passenger Tires"; paper presented to 1967 National Convention,Society for Non-destructive Testing, at Cleveland, Ohio, October 18, 1967.

4. Morris, W.E. et al.,(Research Laboratories, Goodyear Tire and Rubber Company, Akron, Ohio), "Ultrasonic Method of Tire Inspection"; Review of Scientific Instruments, Vol. 23, No. 12, pp. 729-734, December, 1952.

5. Gregory,R.K.,and L.U. Rustrelli, "Nondestructive Inspection Techniques for Aircraft Tires"; Southwest Research Institute Technical Report ASD-TR-68-11, April 1968 (AD856347).

6. Kopel, Le Roy A., "Method of Producing Ultrasonic Energy Absorbing Material," U.S. Patent 3,487,137, December 30, 1969. (assigned to Hewlett-Packard Co.).

7. Papadakis, E.P., and K.A. Fowler, "Broadband Transducers: Radiation Field and Selected Applications"; J. Acoust. Soc. Am., Vol. 50, No. 3, (Part 1), pp. 729-745, 1971.

8. McMaster, R.C.,(editor), Nondestructive Testing Handbook, Ronald Press, New York, (1963).

9. Krautkramer, J. and H. Krautkramer , Ultrasonic Testing of Materials, Springer-Verlag, New York 1969.

10. Lavery, A.L., I. Litant, R.P. Ryan, N. Knable, H.L. Ceccon, "Survey of Non-destructive Tire Inspection Techniques." Department of Transportation, Transportation Systems Center, Cambridge, Ma. Preliminary Memo, Report No. DOT-TSC-NHTSA-71-5, July 1971.

11. Kinsler, L.E. and A.R. Frey, Fundamentals of Acoustics, Wiley, New York, 1950.

12. Frederick, J.R., Ultrasonic Engineering, Wiley, New York, 1965.

13. Fowler, K., Parametrics, Inc., 221 Crescent St., Waltham, Mass. 02154, Private Communication.

14. Martin, E. and K. Werner, Fehler aufzeichnung beim Überschall-Impuls-Laufzeiz-Verfahren, Arch. Eisenhütten wes. 27, p.579-594, (1956).

APPENDIX - ACOUSTIC PROPERTIES OF TIRE MATERIALS

METHOD OF MEASUREMENT

The acoustic impedance and attenuation of a slab of material can be determined by measuring the amplitudes of the reflections from its front surface and from its back surface in comparison with the front interface reflection from a reference standard material of known properties.

For sound normally incident at an interface from medium 1 to medium 2, the amplitude reflection and transmission coefficients are:

$$R_{12} = \frac{Z_2 - Z_1}{Z_2 + Z_1} = \frac{r_{12} - 1}{r_{12} + 1} \qquad \text{(A-1)},$$

$$T_{12} = \frac{2Z_2}{Z_2 + Z_1} = \frac{2r_{12}}{r_{12} + 1} \qquad \text{(A-2)},$$

where $r_{12} = Z_2/Z_1$ is the ratio of the impedance of the second medium relative to that of the first. For an exact calculation, the impedance of a lossy medium is complex. However, for an approximate determination, assuming all impedances are real, comparison of front interface reflections from a reference standard material of known impedance serves to determine the impedance of the sample, using (A-1). With the sample impedance known, equation (A-2) can be used to calculate the transmission losses at the front interface. The additional loss observed for the reflection from the back of the sample is then attributed to attenuation. The magnitude of the attenuation coefficient so determined provides *a posteriori* justification for use of the approximate procedure.

The necessary equations are rewritten in the order and form in which they are used, with appropriate choice of media subscripts, according to the notation defined in figure A-1. The symbols B_s, C_s, B_x, C_x denote the amplitudes of the reflection signals corresponding to the paths indicated in the diagram, while A denotes the unknown amplitude of the incident pulse, which will be eliminated in the derivation.

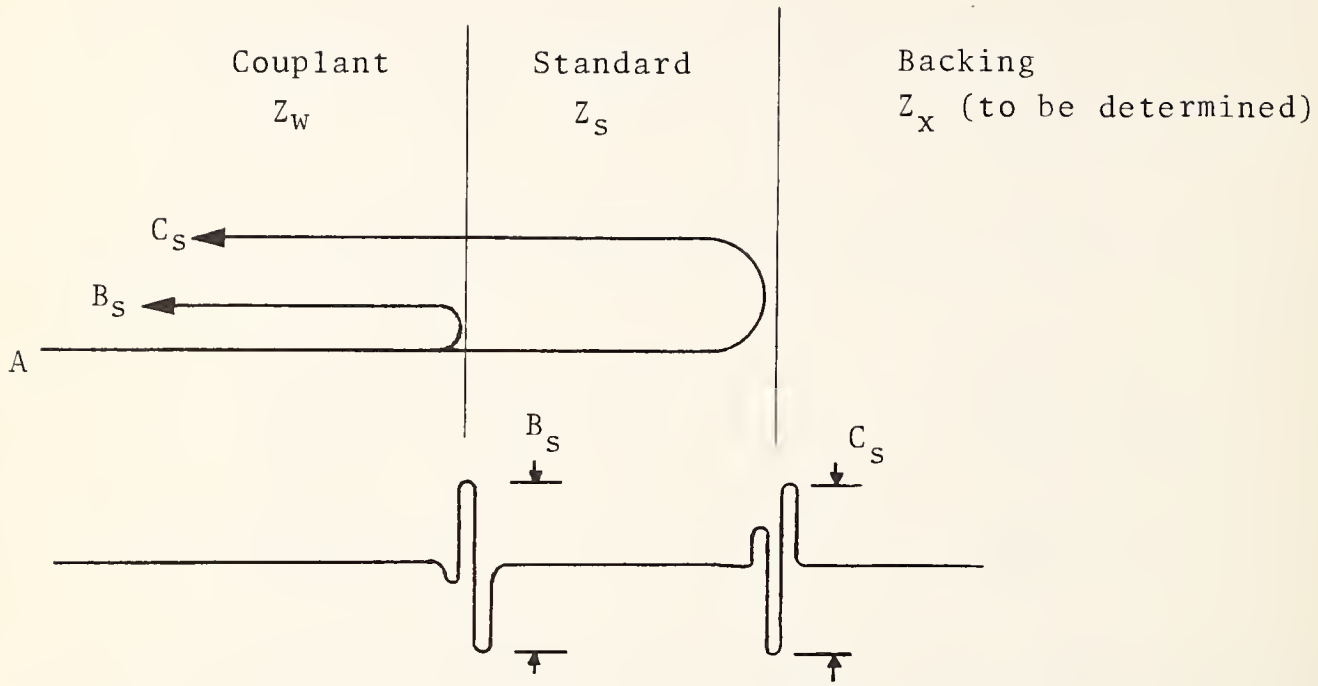

Measurement on Reference Standard

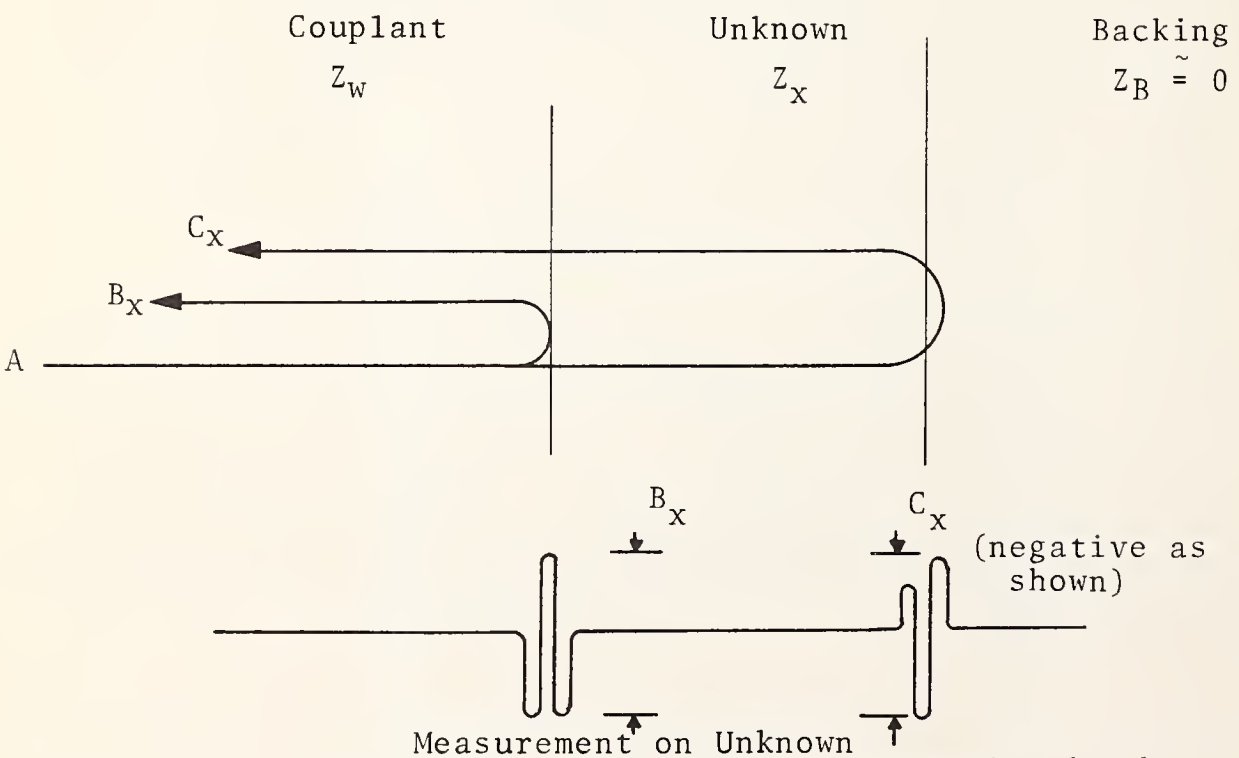

Measurement on Unknown

Figure A-1. Measurements on Reference Standard and Unknown

From known values of Z_w and Z_s, one calculates

$$r_{ws} = Z_s/Z_w \qquad \text{(A-3)}$$

and

$$R_{ws} = \frac{r_{ws}-1}{r_{ws}+1} \quad . \qquad \text{(A-4)}$$

The front interface reflections from the standard and the unknown will be given by multiplying the incident amplitude A by reflection coefficients, i.e.,

$$B_s = A\, R_{ws} \qquad \text{(A-5)}$$

$$B_x = A\, R_{wx} \quad , \qquad \text{(A-6)}$$

and since the incident amplitude A is kept constant for both measurements,

$$R_{wx} = \frac{B_x}{B_s}\, R_{ws} \quad , \qquad \text{(A-7)}$$

in which the value of R_{ws} computed from equation (A-4) is to be used. Using the resulting value for Rwx, equation (A-1) is solved for

$$r_{wx} = \frac{1+R_{wx}}{1-R_{wx}} \quad . \qquad \text{(A-8)}$$

Now the return from the back of the sample is given by

$$C_x = A \{ T_{wx} e^{-\alpha t} R_{xB} e^{-\alpha t} T_{xw} \} \quad , \qquad \text{(A-9)}$$

allowing for transmission through the front interface once in each direction, reflection from the backing, and exponential attenuation while traveling through the sample thickness, t, once in each direction.

In this measurement, the unknown is in dry contact with a sheet cork surface. For an intervening air layer, or even for the cork itself, Zb<<Zx, and to a very good approximation, $R_{xB} = -1$.

Dividing by (A-5)

$$\frac{C_x}{B_s} = \frac{- T_{wx} \; T_{xw} \; e^{-\alpha(2t)}}{R_{ws}} \qquad \text{(A-10)}$$

Substituting from (A-2) in appropriate form, and manipulating gives:

$$\left(\frac{-C_x}{B_s}\right) R_{ws} = \left(\frac{2r_{wx}}{r_{wx}+1}\right) \quad \left(\frac{2r_{xw}}{r_{xw}+1}\right) \quad e^{-\alpha(2t)} , \qquad \text{(A-11)}$$

$$= \frac{4}{(r+1)\left(\frac{1}{r}+1\right)} \quad e^{-\alpha(2t)} , \qquad \text{(A-12)}$$

$$= T_d e^{-\alpha(2t)} , \qquad \text{(A-13)}$$

where $r \equiv r_{wx} \equiv \frac{1}{r_{xw}}$ and we have defined

$$T_d \equiv T_{xw} \, T_{wx} = \frac{4}{(r+1)\left(\frac{1}{r}+1\right)} , \qquad \text{(A-14)}$$

as the amplitude factor associated with the double transit of the couplant/sample interface.

From equation (A-13), the attenuation factor is

$$F \equiv e^{-\alpha(2t)} = \left[\frac{-C_x}{B_s} \; R_{ws}\right] \; / \; T_d . \qquad \text{(A-15)}$$

The loss due to attenuation can be expressed in decibels as

$$L_A[db] = -20 \log \{F\}, \qquad \text{(A-16)}$$

while that due to transmission across the coupling medium interface is

$$L_T = -20 \log \{T_d\} \qquad \text{(A-17)}$$

The attenuation coefficient is then given, in various units:

$$\alpha[\text{Nepers/inch}] = \frac{-\ln\{F\}}{2t[\text{inches}]}, \qquad \text{(A-18)}$$

$$\alpha[\text{dB/inch}] = \frac{-20 \log\{F\}}{2t[\text{inches}]}, \qquad \text{(A-19)}$$

$$\alpha[\text{Nepers/cm}] = \alpha[\text{Nepers/inch}]/2.54, \qquad \text{(A-20)}$$

$$\alpha[\text{dB/cm}] = \alpha[\text{db/inch}]/2.54. \qquad \text{(A-21)}$$